



**HAL**  
open science

## **Pectin modifications in raw fruits alter texture of plant cell dispersions**

Alexandra Buergy, Agnès Rolland-Sabaté, Alexandre Leca, Catherine M.G.C. Renard

► **To cite this version:**

Alexandra Buergy, Agnès Rolland-Sabaté, Alexandre Leca, Catherine M.G.C. Renard. Pectin modifications in raw fruits alter texture of plant cell dispersions. *Food Hydrocolloids*, 2020, 107, pp.105962. 10.1016/j.foodhyd.2020.105962 . hal-02992654

**HAL Id: hal-02992654**

**<https://hal.inrae.fr/hal-02992654>**

Submitted on 20 May 2022

**HAL** is a multi-disciplinary open access archive for the deposit and dissemination of scientific research documents, whether they are published or not. The documents may come from teaching and research institutions in France or abroad, or from public or private research centers.

L'archive ouverte pluridisciplinaire **HAL**, est destinée au dépôt et à la diffusion de documents scientifiques de niveau recherche, publiés ou non, émanant des établissements d'enseignement et de recherche français ou étrangers, des laboratoires publics ou privés.



Distributed under a Creative Commons Attribution - NonCommercial 4.0 International License

# Pectin modifications in raw fruits alter texture of plant cell dispersions

Alexandra Buergy<sup>a</sup>, Agnès Rolland-Sabaté<sup>a, \*</sup>, Alexandre Leca<sup>a</sup>, Catherine M. G. C. Renard<sup>b</sup>

<sup>a</sup> INRAE, Avignon Université, UMR SQPOV, 84914 Avignon, France

<sup>b</sup> INRAE, CEPIA, 44316 Nantes, France

\* Corresponding author.

*E-mail address:* agnes.rolland-sabate@inrae.fr (A. Rolland-Sabaté).

## Abstract

The texture of pureed fruits and vegetables depends primarily on the original tissue structure and cell wall (CW) properties. However, how variations in the raw fruits' cellular and molecular structure determine the rheological behaviour of the purees is little understood, though pectin degradation appears to play a key role. Cultivars, fruit load and post-harvest storage were used to obtain raw apples with different tissue structures, which were processed into purees under simulation of an industrial process. The rheological behaviour of the purees was then compared to particle size, pulp wet mass and serum viscosity. The polysaccharide composition of soluble and insoluble CW material were determined after preparation of alcohol insoluble residue. Macromolecular size and molar mass distributions of soluble pectins were analysed using high performance size-exclusion chromatography coupled to multi-angle laser light scattering and online viscometry. Variations in the raw material, especially induced by post-harvest storage, generated a wide range of different puree's textures. Rheological behaviour of apple purees was driven by particle size, which decreased

26 during prolonged post-harvest storage due to reduced cell adhesion. This was correlated with  
27 pectic side chain hydrolysis and modifications in pectin molar mass and structure. Similar  
28 trends during storage were observed with different apple cultivars and agricultural practices.

29

30 Fruit processing; Apple; Puree; Rheology; Particle size; Polysaccharide

31

## 32 **1. Introduction**

33

34 Purees are manufactured from the edible parts of fruits and vegetables, which are mainly  
35 composed of parenchyma cells. They are dispersions of soft and deformable insoluble  
36 particles (pulp) in an aqueous medium (serum) composed of sugars, organic acids and pectic  
37 polysaccharides (Rao, 1992). The pulp is primarily composed of cell wall clusters, individual  
38 cells whose content was emptied during puree processing or cell fragments from the  
39 parenchyma of the original fruit, ranging between some mm and some hundred  $\mu\text{m}$  in size  
40 (Espinosa et al., 2011; Leverrier, Almeida, Espinosa-Munoz, & Cuvelier, 2016). In apple  
41 fruits, parenchyma cells are polyhedral in shape and between 50 and 300  $\mu\text{m}$  in diameter  
42 (Khan & Vincent, 1990).

43 In reconstituted model systems, the amount, size and shape of individual cells or cell clusters  
44 as well as the viscosity of the serum are reported to be key factors in determining the puree's  
45 texture (Espinosa-Munoz, Renard, Symoneaux, Biau, & Cuvelier, 2013; Espinosa et al., 2011;  
46 Leverrier, Almeida, Espinosa-Munoz, & Cuvelier, 2016; Rao, 1992), and are all closely  
47 linked to the quality of pectic polysaccharides. However, to the best of our knowledge, no  
48 extensive study investigated the relationship between quality variations of raw apples, linked  
49 to pectins, and texture of corresponding purees. In contrast, the evolution of pectic substances  
50 in raw apples is well documented. For example, fruit cultivar as well as maturity stage modify

51 the chemical and structural properties of the cell wall (Billy et al., 2008; Fischer & Amado,  
52 1994; Le Bourvellec et al., 2011).

53 The main compartment of parenchyma cells is the large central vacuole, surrounded by the  
54 gel-like cytoplasm. The thin (0.1 to 10  $\mu\text{m}$ ) and semi-rigid cell wall, containing cellulose,  
55 hemicellulose and pectins, is located around this complex and plays an important role as it  
56 assures structural support to the plant cell (Darvill, McNeil, Albersheim, & Delmer, 1980).  
57 The colloidal middle lamella is situated between the primary cell walls of adjacent cells,  
58 holding them together and thus, forming the tissue (Thakur, Singh, & Handa, 1997). The  
59 middle lamella is almost only composed of pectic polysaccharides, accompanied by proteins  
60 (Carpita & Gibeaut, 1993) but without cellulose (Guillemin et al., 2005).

61 Pectin molecules are a group of different complex polysaccharides rich in covalently linked  
62 D-galacturonic acid that form a negatively charged backbone (Albersheim, Darvill, Oneill,  
63 Schols, & Voragen, 1996). The homogalacturonans (HG) are composed of a long, linear chain  
64 of  $\alpha\text{-D-(1} \rightarrow 4\text{)-galacturonic acids}$ . These regions do not carry any neutral sugars as side  
65 chains but the galacturonic acid residues can be methyl esterified to a varying degree at C6  
66 positions, defining the degree of methylation (DM) (Thakur, Singh, & Handa 1997).  
67 Depending on the DM, HG chains may self-associate; an unmethylated C-6 position of the  
68 HG backbone is negatively charged and may ionically interact with calcium-ions to form a  
69 stable gel with other HG molecules if more than 10 consecutive unmethyl-esterified  
70 galacturonic acid residues are coordinated (Kohn & Luknár, 1977). In the  
71 rhamnogalacturonan I (RG I) backbone,  $\alpha\text{-D-(1} \rightarrow 4\text{)-galacturonic acid}$  and  $\alpha\text{-L-(1} \rightarrow 2\text{)-}$   
72 linked rhamnose molecules residues alternate, whereas the rhamnosyl residues can be  
73 substituted with neutral sugar chains. These lateral chains can be linear or branched and are  
74 mainly composed of  $\alpha\text{-L-arabinofuranosyl}$  and/or  $\beta\text{-D-galactopyranosyl}$  forming arabinans,  
75 galactans and arabinogalactans (Ridley, O'Neill, & Mohnen, 2001). Rhamnogalacturonan II

76 (RG II) molecules consist of a galacturonic acid backbone, carrying four complex  
77 oligosaccharide chains consisting of 12 different glycosyl residues in over 20 different  
78 linkages (Mohnen, 2008). *In muro*, RG II exists predominantly as a dimer that is cross-linked  
79 by a borate-diol ester (O'Neill et al., 1996).

80 During processing into puree, rising temperatures destabilize cellular membranes and favour  
81 both enzymatic and chemical reactions, resulting in degradation and solubilization of pectic  
82 polysaccharides that are involved in cell-to-cell adhesion (Massiot & Renard, 1997). The  
83 tissue is then softened due to increased cell separation. In addition, mechanical treatment  
84 partly disrupts the parenchyma cells that release their cell content.

85 Due to the increasing number of consumers and purchased quantities of fruit purees, food  
86 companies are highly interested in predicting and controlling the puree's texture since this is a  
87 major quality attribute and thus a key for the liking and, in turn, repeated purchase of the  
88 products (Waldron, Smith, Parr, Ng, & Parker, 1997). However, fruit purees may need to be  
89 rectified by concentration, addition of sugar or hydrocolloids, which may be perceived  
90 negatively by consumers. Thus, there is a global trend towards the production of healthier and  
91 more natural fruit products and the reduction of artificial stabilizers or texturizing agents  
92 (Market Research Future, 2019). This could be reached by playing on the structural factors of  
93 the raw fruit, as it is known, but not mastered by industry, that texture of plant-based products  
94 highly depends on the cell wall structure of the raw material (Waldron, Smith, Parr, Ng, &  
95 Parker, 1997).

96 The objective of this study was thus to identify the impact of pectin structure in raw apples on  
97 texture variations of the corresponding purees. To reach this aim, two apple cultivars, four  
98 post-harvest storage durations and two growing conditions were chosen to generate contrasted  
99 raw apples. Their impact on the structural factors as well as the cell wall composition of the  
100 apple purees was studied in order to relate microstructure to the puree's texture.

101

## 102 **2. Material and Methods**

103

### 104 *2.1. Plant material*

105

106 Apple (*Malus domestica* Borkh.) cultivars, namely ‘Granny Smith’ and ‘Golden Delicious’  
107 were cultivated in Mallemort, France and harvested in September 2017 according to the  
108 optimal harvest dates. ‘Granny Smith’ (GS) and half of the trees of the cultivar ‘Golden  
109 Delicious’ (GD) were thinned chemically (GD1), leading to less but bigger fruits ( $201 \pm 7$  g  
110 per apple). GS trees showed regular fruit growth and were thus thinned with 600 g/ha Amid-  
111 Thin® W (2-(1-naphthyl)acetamide) and 1 kg/hL Rhodofix® (1-naphthalenacetic acid). GD1  
112 trees exhibited low fruit charge and were thus treated with 15 L/ha ammonium thiosulfate and  
113 0.15 kg/hL Rhodofix®. Additionally, 3.5 L/ha MaxCel® (6-Benzylaminopurine) were applied  
114 on small fruits of both varieties. The other half of GD trees was not thinned (GD2), resulting  
115 in more but smaller fruits ( $176 \pm 4$  g per apple). The raw apples used in this article were  
116 characterized in detail (e.g. fruits’ texture) in another study (Lan, Jaillais, Leca, Renard, &  
117 Bureau, 2020).

118 A first series of samples were processed directly after harvest (T0). The apples were then  
119 stored for one (T1), three (T3) and six (T6) months at 4 °C prior to processing. The  
120 atmosphere was not controlled to allow post-harvest storage to have significant impact.

121

### 122 *2.2. Puree preparation*

123

124 For each cultivar, growth condition and storage time, processing was conducted in triplicate.

125 Approximately 3 kg of apple fruits per batch were cored, sliced into 12 equal portions and

126 processed into puree. A cooker-cutter (RoboQbo Qb8-3, RoboQbo, Bentivoglio, Italy) was  
127 used for apple processing, imitating a hot break process at 95 °C, with stirring at 105 rad/s  
128 during five minutes under vacuum. Each batch of apple puree was divided into two portions:  
129 one was refined by an automatic sieve (Cobot Coupe C80, Robot Coupe SNC, Vincennes,  
130 France) of 0.5 mm (R), removing skin and other larger particles, and the other one was not  
131 refined (NR). At T0, only NR samples were produced. Rheological measurements, particle  
132 size analysis and determination of pulp wet mass were conducted in the same week as puree  
133 preparation. Pulp and serum were then frozen separately (-20 °C) until cell wall extraction  
134 and analysis.

135

### 136 *2.3. Rheological measurements*

137

138 All tests were performed using a stress-controlled rheometer (Physica MCR301, Anton Paar,  
139 Graz, Austria) equipped with a Peltier cell (CPTD-200, Anton Paar) and an external cylinder  
140 (CC27/S, Anton Paar). All rheological measurements were performed at 22.5 °C and samples  
141 were changed for each test.

142

#### 143 *2.3.1. Puree*

144 A vane measuring system with a 3.46 mm gap (CC27/S + FL100/6W, Anton Paar) was used  
145 to analyse the rheological behaviour of the purees. The flow curve was recorded by measuring  
146 the viscosity over a logarithmically distributed range of shear rate values  $\dot{\gamma}$  between 10 and  
147 250 s<sup>-1</sup>. One point was recorded every 15 seconds. Homogenous dispersion of the product in  
148 the measurement cell was ensured by application of a pre-shear of 50 s<sup>-1</sup> during two minutes,  
149 followed by a five minute rest to let the puree return to a rheological equilibrium prior to  
150 analysis. The texture of the purees was compared by means of the apparent viscosity ( $\eta_{app}$ ) at

151 a shear rate of  $50 \text{ s}^{-1}$  as this value represents an approximation of the shear rate to which a soft  
152 food product is subjected in the mouth during mastication (Stokes, 2012).

153 Amplitude sweep tests were performed at deformation values  $\gamma$  between 0.01 and 100 % at a  
154 fixed angular frequency  $\omega$  of 10 rad/s. Five points were measured per decade and the time  
155 required to measure each point was set by the software. The yield stress obtained at the  
156 intersection of  $G'$  and  $G''$  was used as a characteristic point to estimate the minimum shear  
157 stress that must be applied to the puree to initiate flow (Espinosa-Munoz, Renard,  
158 Symoneaux, Biau, & Cuvelier, 2013). The values of  $G'$  and  $G''$  were averaged in the linear  
159 viscoelastic range. The end of the linear domain was estimated as the strain inducing a  
160 decrease of  $G'$  values **exceeding** 10 % of its value in the linear domain.

161 The method used for rheological measurements of the purees was theoretically not adapted for  
162 particles larger than 1 mm as the gap of the measuring cell was approximately 3 mm large.  
163 **The only samples containing particles (skin fragments) larger than 1 mm were not refined**  
164 **purees. However, rheological measurements were repeatable for these samples and the**  
165 **method was thus considered valid.**

166

### 167 2.3.2. Serum

168 The viscosity of the continuous phase obtained by centrifugation of the puree was measured  
169 using a double gap cylinder geometry (DG27, Anton Paar). Before each measurement, a  
170 resting step of one minute was applied. Viscosity values ( $\eta_{\text{serum}}$ ) were taken at a shear rate of  
171  $100 \text{ s}^{-1}$  from a flow curve, assuming the in-mouth perception of serum requires a higher shear  
172 rate than purees.

173

### 174 2.4. Pulp wet mass

175



176 The pulp wet mass represented the fraction of humid particles after separation of the puree  
177 into pulp and serum by centrifugation at 7690 x g for 15 minutes at 15 °C. It was calculated as  
178 the ratio of the pulp weight to the initial weight of the puree and expressed in % as described  
179 in literature (Espinosa-Munoz, Renard, Symoneaux, Biau, & Cuvelier, 2013).

180

### 181 2.5. Particle size distribution

182

183 The particle size distribution of the pulp was measured by laser granulometry (Mastersizer  
184 2000, Malvern Instruments, Malvern, UK). The samples were dispersed in distilled water  
185 (refractive index: 1.33) and analysed by the Mie theory. The refractive index of the sample  
186 was set at 1.52 (Leverrier, Almeida, Espinosa-Munoz, & Cuvelier, 2016) and the absorptive  
187 index was chosen to be 0.00 due to the translucent character of apple cells. Each sample was  
188 analysed in duplicate and the Malvern's software averaged the size distribution over three  
189 repeated measurements on the same sample.

190

### 191 2.6. Alcohol insoluble solids (AIS)

192

193 AIS of raw apples and purees were extracted as described by Le Bourvellec et al. (2011). AIS  
194 of serum and pulp were prepared based on Renard (2005) and Le Bourvellec et al. (2011).  
195 Prior to cell wall extraction, pulp was water-washed to remove soluble pectins.  
196 Approximately 25 g of fresh pulp were suspended in ultrapure water (130 mL), then stirred  
197 one night (10 rad/s, 4 °C) and centrifuged (7690 x g, 10 min, 15 °C). The residue was rinsed  
198 once again with water before 10 g of the sediment were stirred (10 rad/s, 4 °C) one night in  
199 ethanol (96 % v/v, 50 mL). The suspension was filtered on a 75 mL Sep-pack column  
200 (Interchim, Montluçon, France) equipped with a 20 µm filter. The extraction was continued

201 with ethanol (70 % v/v) till absence of sugars as shown by negative reaction in the phenol  
202 sulphuric test (Dubois, Gilles, Hamilton, Rebers, & Smith, 1956). Subsequently, the samples  
203 were washed twice with acetone (60 % v/v), once with acetone (80 % v/v) and three times  
204 with acetone (100 % v/v). The residue was dried at 40 °C during 48 hours in a drying oven  
205 and weighed. The cell wall content of the pulp was estimated as the relation between the dry  
206 pulp weight and the initial pulp weight after water-washing, expressed in %.

207 For serum, 100 mL were stirred (31 rad/s, 4 °C) overnight in 250 mL ethanol (96 % v/v), then  
208 centrifuged (7690 x g, 15 °C, 10 minutes). The residue was washed several times with ethanol  
209 (70 % v/v) until all free sugars were removed. Afterwards, samples were dissolved in water  
210 (50 mL) overnight (31 rad/s, 4 °C) to redissolve the pectins, then freeze-dried and ground  
211 with an *All basic* batch mill (IKA, Staufen, Germany). A rough estimation of the soluble  
212 pectin content can be calculated by the relation between the samples' weight after freeze-  
213 drying and the initial weight of 100 mL serum, expressed in %.

214

## 215 *2.7. Water retention capacity*

216

217 The water retention capacity of the pulp was calculated as the amount of water retained by the  
218 mass of the pulp's AIS (g/g dry weight) according to Robertson et al. (2000). In this study, it  
219 was estimated as the relation between the pulp wet mass and the mass of the pulp's AIS. The  
220 mass of the fibre is generally negligible and was thus not considered in this equation.

221

## 222 *2.8. Sugar composition of AIS*

223

### 224 *2.8.1. Cell wall analysis*

225 AIS (10 mg) were subjected to prehydrolysis with sulphuric acid (72 % v/v) for one hour at  
226 room temperature. Afterwards, the samples were diluted to 1 M sulphuric acid by addition of  
227 water and internal standard (inositol) and heated at 100 °C for 3 hours (Saeman, Moore,  
228 Mitchell, & Millett, 1954). For neutral sugars analysis, the free sugars were derivatized to  
229 volatile alditol acetates according to the method described by Englyst, Wiggins, and  
230 Cummings (1982). They were injected on a Clarus 500 gas chromatograph (PerkinElmer,  
231 Waltham, USA) equipped with a flame ionization detector (FID) and a OPTIMA® capillary  
232 column of 30 m × 0.25 mm i.d. and 0.25 µm film thickness (Macherey-Nagel, Düren,  
233 Germany). Helium was used as carrier gas at 1.5 mL/min and the injector temperature was set  
234 at 250 °C in split mode (ratio 1:8). The oven temperature was maintained at 230 °C.

235 Galacturonic acid was measured spectrophotometrically by the m-hydroxydiphenyl assay  
236 (Blumenkrantz & Asboe-Hansen, 1973) in the acid hydrolysates.

237 Methanol was quantified via stable isotope dilution assay after saponification (Renard &  
238 Ginies, 2009) on a *Trace 1300* gas chromatograph (Thermo Scientific, Waltham, USA) and a  
239 coupled *ISQ LT* single quadrupole mass spectrometer (Thermo Scientific, Waltham, USA).  
240 Capillary column was a TG-WaxMS of 30 m × 0.25 mm i.d. and 0.5 µm film thickness.  
241 Samples' headspace was injected in split injector (ratio 15:1) at 220 °C. Helium (70 kPa) was  
242 used as carrier gas. The oven temperature was set at 40 °C. Electron ionization (70 eV) was  
243 used at 250 °C.

244 The degree of methylation (DM) was calculated as molar ratio of methanol to galacturonic  
245 acid and expressed in %.

246

#### 247 2.8.2. Starch determination

248 Starch was quantified in the AIS of the pulp, serum and raw apples using the total starch assay  
249 kit K-TSTA (Megazyme, Wicklow, Ireland) according to the manufacturer's instructions

250 except that the amount of enzymes was doubled to **counteract** enzyme inhibition by the  
251 interaction of remaining polyphenols in the AIS with the enzymes. The test was performed in  
252 duplicate. All values for AIS, neutral sugars, galacturonic acid and methanol were corrected  
253 by the respective starch content in the sample.

254

255 *2.9. High performance size-exclusion chromatography coupled to multi-angle laser light*  
256 *scattering (HPSEC-MALLS) and online viscometry*

257

258 Molar mass and size distributions of soluble pectins was obtained by HPSEC-MALLS  
259 coupled to viscometric detection. An Ultra Fast Liquid Chromatography Prominence system  
260 (Shimadzu, Kyoto, Japan) including a LC-20AD pump, a DGU-20A5 degasser, a SIL-  
261 20AUCHT autosampler, a CTO-20 AC column oven, a SPD-M20A diode array detector and a  
262 RID-10A refractive index detector from Shimadzu (Tokyo, Japan) was employed together  
263 with a multi-angle laser light scattering detector (DAWN HELEOS 8+ fitted with a K5 flow  
264 cell and a GaAs laser,  $\lambda = 660$  nm) and a ViscostarIII viscometer from Wyatt Technology  
265 Corporation (Santa Barbara, CA). Three HPSEC columns (PolySep-GFC-P3000, P5000 and  
266 P6000 300  $\times$  7.8 mm) and a guard column from Phenomenex (Le Pecq, France) were used for  
267 the separation and all the HPSEC-MALLS system was maintained at 40 °C. The eluent, an  
268 acetate buffer (0.2 M) at pH 3.6, was carefully filtered through a 0.1  $\mu$ m omnipore™  
269 membrane from Millipore (Milford, USA) and degassed before elution at a flow rate of  
270 0.6 mL/min for 130 minutes. Pectins were solubilized overnight under magnetic stirring  
271 directly in the filtered eluent at 4 °C to a theoretical concentration of 10 mg AIS/mL (raw  
272 apples) and 2.5 mg AIS/mL (serum). The samples were centrifuged (7690 x g, 4 °C, 10  
273 minutes) and the supernatant was filtered through 0.45  $\mu$ m hydrophilic PTFE syringe filter  
274 (Macherey-Nagel, Düren, Germany) before injection (100  $\mu$ L). ASTRA® software from

275 Wyatt Technology Corporation (version 7.1.4 for PC) was used to establish  $M_i$  and  $R_{gi}$ , the  
276 molar mass and the radius of gyration at the  $i^{\text{th}}$  slice of the chromatogram using the light  
277 scattering signal from six angles ( $20.4^\circ$ - $110^\circ$ ) and the Zimm formalism with a one order  
278 polynomial fit to extrapolate the data to zero angle (Rolland-Sabaté, Colonna, Potocki-  
279 Véronèse, Monsan, & Planchot, 2004). ASTRA<sup>®</sup> software was also used to calculate the  
280 viscometric hydrodynamic radius for the equivalent sphere by combining viscosity and molar  
281 mass measurements using the following equation derived from the Einstein and Simha  
282 relation (Einstein, 1906, 1911; Simha, 1940):

283

$$284 \quad [\eta]_i M_i = \gamma N_A V_{hi} = \frac{10\pi}{3} N_A R_{hi}^3 \quad (1)$$

285

286 where  $[\eta]_i$ ,  $R_{hi}$  and  $V_{hi}$  are the intrinsic viscosity, the hydrodynamic radius and the  
287 hydrodynamic volume at the  $i^{\text{th}}$  slice of the chromatogram,  $\gamma = 2.5$  for spheres and  $N_A$  is the  
288 Avogadro number. The weight-average molar mass  $\bar{M}_w$ , the z-average radius of gyration  $\bar{R}_{gz}$ ,  
289 the z-average intrinsic viscosity  $[\bar{\eta}]_z$  and the z-average viscometric hydrodynamic radius  
290  $\bar{R}_{hz}(v)$  were obtained by taking the summations over the whole peaks. The refractive index  
291 increment (dn/dc) for glycans was fixed at 0.146 mL/g and the normalization of photodiodes  
292 was achieved using a low molar mass pullulan standard (P20) from Showa Denko K.K.  
293 (Tokyo, Japan).

294

### 295 2.10. Statistical analysis

296

297 The Shapiro-Wilk test showed that not all data were normally distributed. Therefore, they  
298 were assessed by Kruskal-Wallis non-parametric test (Kruskal & Wallis, 1952) using R  
299 statistical software (R Core Team, 2018). Here, the H value is the test statistic that is used to

300 calculate the P values. Differences were considered to be significant at  $P < 0.05$ . Standard  
301 deviations were calculated for each series of replicated measurement using the sum of  
302 individual variances weighted by the individual degrees of freedom (Box, Hunter, & Hunter,  
303 1978). Principal Component Analysis (PCA) was performed using the package “FactoMineR”  
304 (Lê, Josse, & Husson, 2008) for R statistical software.

305

### 306 **3. Results and discussion**

307

#### 308 *3.1. Rheological parameters of apple purees*

309

310 All apple purees showed a shear-thinning behaviour (data not shown) as already described  
311 (Espinosa et al., 2011; Rao, Cooley, Nogueira, & McLellan, 1986). Apple cultivar and tree  
312 thinning practice (summarized as “raw material”, Table 1) led to significantly different  
313 puree’s viscosities. The highest values were obtained for GD1 and the lowest for GD2 (Fig.  
314 1A). The apparent viscosity of the purees ( $\eta_{app}$ ) also changed significantly with post-harvest  
315 storage (Table 1). However, this change did not follow a monotonous tendency, as for GD  
316 (GD1 and GD2) the viscosity decreased during the first months of post-harvest storage before  
317 increasing again between three and six months. For GS, however,  $\eta_{app}$  decreased  
318 monotonously for not refined samples during storage whereas viscosity of refined samples  
319 increased (Fig. 1A). The refined purees showed significantly lower viscosity values than not  
320 refined samples which might be explained by particle size.

321 Different apple cultivars and fruit loads also generated significantly different yield stress  
322 values (Table 1), the highest for GD2 and the lowest for GS (Fig. 1B). For GD apples, yield  
323 stress decreased abruptly between purees prepared from directly harvested apples and purees  
324 made from apples stored for one month. Interestingly, yield stress values from purees

325 obtained from GD at the two fruit loads converged between three and six months. During  
326 post-harvest storage, the yield stress showed similar tendencies as apparent viscosity as a  
327 minimum was observed after three months for GD1, GD2 and not refined GS samples.  
328 Refined GS purees showed continuously increasing yield stress values. Unlike apparent  
329 viscosity, yield stress was not significantly affected by refining (Table 1).

330

### 331 *3.2. Structural parameters of apple purees*

332

#### 333 *3.2.1. Serum viscosity*

334 Highest values of serum viscosity (Fig. 1C) were obtained with GS and the lowest with GD2,  
335 except at T6. Even if serum viscosity of GS decreased markedly between T0 and T1, no  
336 significant variations were detected over post-harvest storage (Table 1). Interestingly, the  
337 purees showing the highest serum viscosities revealed the lowest yield stress values. This  
338 might be due to the lubricant effect of the serum as stated by Espinosa-Munoz, Renard,  
339 Symoneaux, Biau, and Cuvelier (2013), even if this trend was only observed for purees  
340 prepared with freshly harvested apples. It was hypothesized that pectins' characteristics, such  
341 as chemical structure and molar mass, were modified over storage so that the lubricant effect  
342 of the serum became less important. Refining did not influence the viscosity of the soluble  
343 phase.

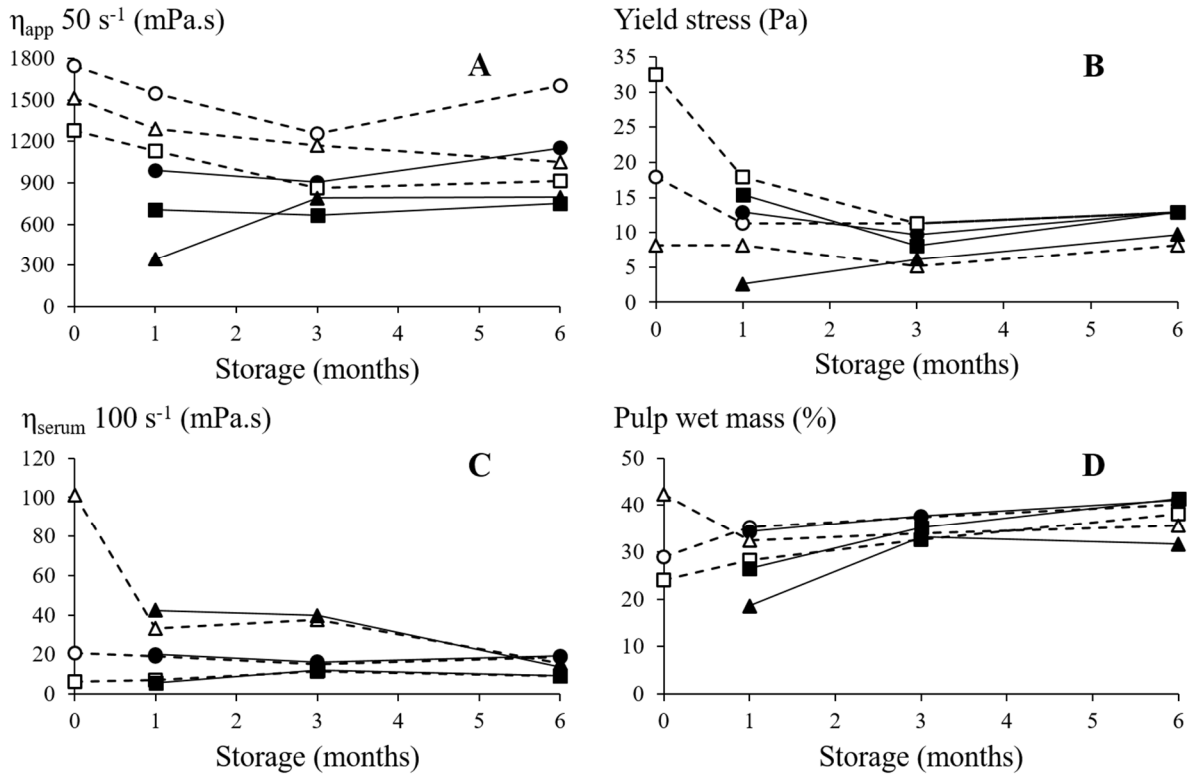
344

#### 345 *3.2.2. Pulp wet mass*

346 For GD apples, pulp wet mass (Fig. 1D) increased significantly over post-harvest storage.  
347 However, for GS, the pulp wet mass decreased strongly during the first month of post-harvest  
348 storage, then increased again. The contrasted trends between the two cultivars could be due to  
349 differences in the cell wall structure, leading to different water retention capacities. Generally,

350 refining did not induce differences in pulp wet mass, though the not refined samples contained  
 351 skin particles.

352



353

354 **Fig. 1.** Rheological and structural parameters of apple purees in function of post-harvest  
 355 storage duration: Apparent viscosity at 50 s<sup>-1</sup> (A), yield stress (B), serum viscosity at 100 s<sup>-1</sup>  
 356 (C), pulp wet mass (D).

357 Round symbols represent GD1, rectangular symbols GD2 and triangular symbols GS. Empty  
 358 symbols display not refined and filled symbols refined (0.5 mm) samples.

359

360

361

362

363

364



365 **Table 1**

366 Kruskal-Wallis *H*-values and *P*-values performed on apparent viscosity at 50 s<sup>-1</sup> ( $\eta_{app}$ ), yield  
 367 stress, serum viscosity at 100 s<sup>-1</sup> ( $\eta_{serum}$ ) and pulp wet mass (% Pulp).

	$\eta_{app}$ 50 s <sup>-1</sup> (mPa.s)	Yield stress (Pa)	$\eta_{serum}$ 100 s <sup>-1</sup> (mPa.s)	% Pulp (%)
Raw material <i>H</i>	16	34	45	7
Raw material <i>P</i>	<b>&lt; 0.05</b>	<b>&lt; 0.05</b>	<b>&lt; 0.05</b>	<b>&lt; 0.05</b>
Storage <i>H</i>	16	12	3	20
Storage <i>P</i>	<b>&lt; 0.05</b>	<b>&lt; 0.05</b>	0.41	<b>&lt; 0.05</b>
Refining <i>H</i>	34	2	1	0
Refining <i>P</i>	<b>&lt; 0.05</b>	0.17	0.31	0.93

368

369 *3.2.3. Particle size distribution*

370 As a representative example, Fig. 2 shows the evolution of particle size distribution during  
 371 post-harvest storage for GD2. Directly after harvest (T0), purees showed a single peak around  
 372 1000  $\mu$ m representing cell clusters (Espinosa-Munoz, Renard, Symoneaux, Biau, & Cuvelier  
 373 2013; Leverrier, Almeida, Espinosa-Munoz, & Cuvelier, 2016). Refining eliminated some  
 374 large particles and the peak shifted to particle sizes close to 800  $\mu$ m. Although a screen  
 375 opening of 0.5 mm was used for refining, particles bigger than 0.5 mm were detected,  
 376 probably because these flexible and deformable particles (Leverrier, Moulin, Cuvelier, &  
 377 Almeida, 2017) could be pressed through the openings.

378 After one month of post-harvest storage, a second peak around 200  $\mu$ m appeared for not  
 379 refined samples. Espinosa-Munoz, Renard, Symoneaux, Biau, and Cuvelier (2013) and  
 380 Leverrier, Almeida, Espinosa-Munoz, and Cuvelier (2016) attributed this peak to individual  
 381 cells by confocal and light microscopy, respectively. Refined samples still showed a  
 382 monomodal size distribution with a broader peak compared to T0, near 500  $\mu$ m. Smaller  
 383 particles in refined purees were in line with lower viscosity values (Fig. 1A) as described in  
 384 literature (Espinosa et al., 2011; Schijvens, van Vliet, & van Dijk, 1998).

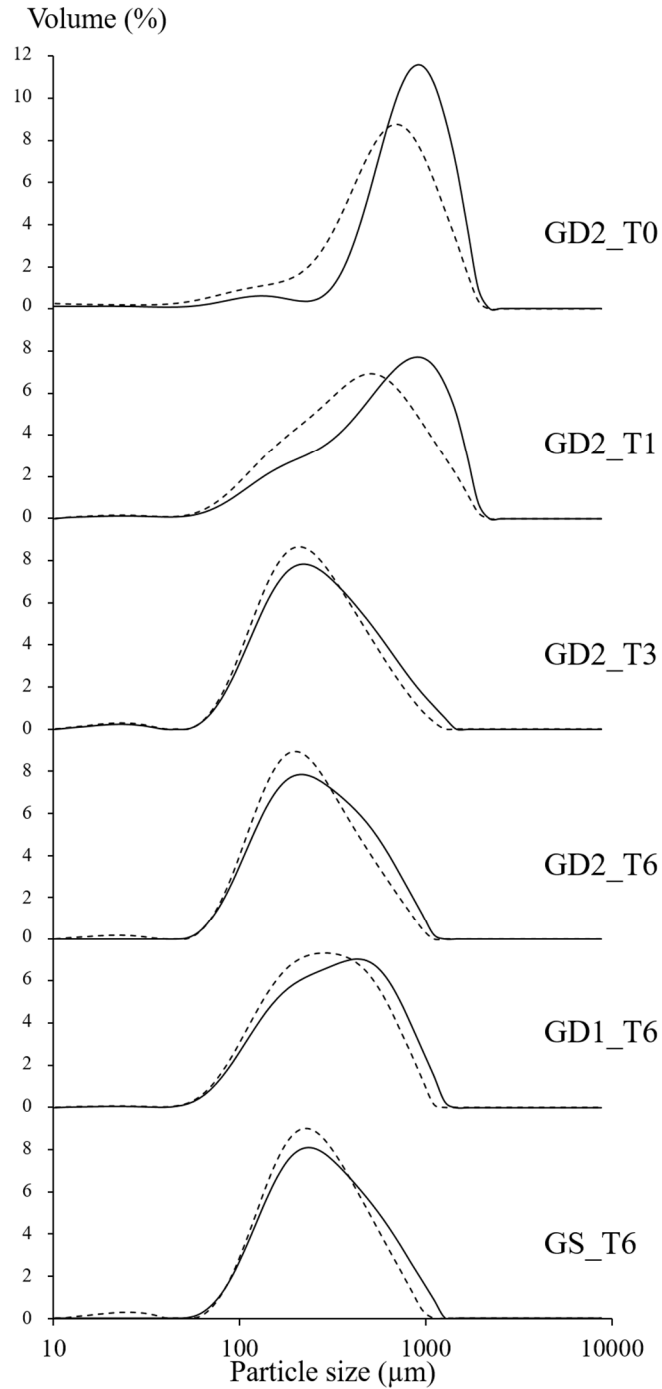
385 At three and six months of post-harvest storage, the particle size remained stable and both the  
386 refined and not refined purees showed a similar size distribution with a main peak around  
387 200  $\mu\text{m}$ . The size and amount of cell clusters in apple purees thus decreased over post-harvest  
388 storage to individual cells. This could be explained by reduced cell adhesion due to pectin  
389 solubilization in the middle lamella by pectinase activity (Koziol, Cybulska, Pieczywek, &  
390 Zdunek, 2017). Thus, a prolonged storage period led to softer tissues, which could be  
391 fragmented more easily during processing.

392 A remarkable result was the convergence of the particle size of not refined and refined purees  
393 over storage time. Consequently, refining of apple purees had limited effect after three months  
394 of post-harvest storage as the particles were already very small after processing. The same  
395 results were obtained with GD1 and GS (data not shown). The texture of refined and not  
396 refined purees was, however, still different after three or six months of post-harvest storage  
397 (Fig. 1A). Fragments of apple skin remained in not refined samples, and thus increased the  
398 apparent viscosity of these samples, but were too big to be detected by laser granulometry.

399 Particle size analysis also revealed differences depending on the apple cultivar and fruit load  
400 (Fig. 2). Between three and six months of post-harvest storage, particle size was stable for GD  
401 purees but still decreased slightly for GS samples (data not shown). Therefore, a plateau  
402 seemed to be reached after six months of post-harvest storage, which was used to compare the  
403 particle size of different apple cultivars and fruit loads. Fruit thinning enhances cell division  
404 (Goffinet, Robinson, & Lakso, 1995) and, depending on apple cultivar and thinning treatment,  
405 cell expansion (Milić et al., 2017; Wismer, Proctor, & Elfving, 1995). Purees of thinned GD1  
406 apples revealed bigger particles than GD2, being in accordance with literature (Milić et al.,  
407 2017). GS apples were also thinned but showed a similar particle size distribution as GD2.  
408 This could be due to varietal effects, which do not respond in the same way to fruit thinning.

409 It is also pointed out that GS and GD1 apples were not thinned with the same chemicals and  
410 the same dose as the trees of these varieties initially possessed different fruit loads.

411 Interestingly, GD1 purees, revealing the biggest particles, also showed the highest viscosity  
412 value after six months of post-harvest storage (Fig. 1A). For GD1 and GD2, apparent  
413 viscosity of the purees decreased until three months of post-harvest storage, which was in line  
414 with a decreasing particle size. Apparent viscosity then increased from three to six months of  
415 post-harvest storage, while particle size remained unchanged. In this case, the puree's texture  
416 was determined by pulp wet mass as it was the only structural factor that increased during  
417 post-harvest storage (Fig. 1D). The apparent viscosity of not refined GS samples decreased  
418 monotonously during post-harvest storage, which was in line with continuously decreasing  
419 particle sizes. Consequently, particle size was the most important factor determining puree's  
420 texture in this experiment. Pulp wet mass appeared to be the second most important factor as  
421 it affected texture only when particle size between two or more purees were the same.



422

423 **Fig. 2.** Particle size distribution of the purees issued from different apple cultivars and at  
 424 different post-harvest maturity stages. GD1: Golden Delicious, reduced fruit load; GD2:  
 425 Golden Delicious, high fruit load; GS: Granny Smith; T0: Directly after harvest; T1: After 1  
 426 month of post-harvest storage; T3: After 3 months of post-harvest storage; T6: After 6 months  
 427 of post-harvest storage; Continuous lines represent not refined purees and dashed lines refined  
 428 (0.5 mm) purees.

429 The key factors determining puree's texture are particle size, insoluble cell wall content and  
430 serum viscosity and are all strongly linked to the cell wall (CW) composition and tissular  
431 structure. Hence, the composition of CW polysaccharides as well as pectins' macromolecular  
432 characteristics in raw fruits and purees were examined in the following sections.

433

### 434 *3.3. Composition of cell wall polysaccharides*

435

436 Table 2 summarizes the yields and compositions of the AIS of raw apples (FR), pulp (PL) and  
437 serum (SE). Puree results are not shown given that Le Bourvellec et al. (2011) described only  
438 minor modifications in CW polysaccharides from raw apples into puree during processing.  
439 Post-harvest storage was identified as the factor inducing the most significant changes in CW  
440 polysaccharides compared to raw material or refining. Consequently, for legibility, Table 2  
441 only shows the evolution of cell wall polysaccharides and starch during post-harvest storage  
442 for not refined samples, averaged for GS, GD1 and GD2. The whole dataset can be found in  
443 Supplementary Table S1.

444 AIS composition of raw apples (Table 2) is consistent with previous studies (Fischer &  
445 Amado, 1994; Le Bourvellec et al., 2011; Massiot & Renard, 1997; Renard, 2005), i.e.  
446 presence of cellulose, highly methylated pectins rich in xylogalacturonans and hemicelluloses  
447 fucogalactoxyloglucans and mannans. The AIS content of raw apples decreased over post-  
448 harvest storage. The same trend was observed by Fischer and Amado (1994) and the values  
449 were similar to those found in literature (15-27 mg/g FW) (Colin-Henrion, Mehinagic,  
450 Renard, Richomme, & Jourjon, 2009; Le Bourvellec et al., 2011; Massiot & Renard, 1997;  
451 Renard, 2005). The main sugars found in the AIS of raw apples were glucose and galacturonic  
452 acid, corresponding to cellulose and pectins, respectively. The glucose content (corrected for  
453 starch) was not altered by storage duration, whereas galacturonic acid slightly increased and

454 arabinose and galactose decreased. Arabinose and galactose are part of the side chains of RG I  
455 and showed the highest values after glucose and galacturonic acid. A decrease of pectin side  
456 chains is a common feature in stored fruits, observed for apples and many other fruits such as  
457 tomatoes, pears and strawberries (Fischer & Amado, 1994; Gross & Sams, 1984; Gwanpua et  
458 al., 2014). Rhamnose did not evolve during post-harvest storage. Xylose showed a slight but  
459 significant increase that has already been observed by Fischer and Amado (1994) and that  
460 might be attributed to the decrease of the neutral sugars arabinose and galactose, resulting in a  
461 relatively higher amount of xylose. Together with fucose and some galactose and glucose,  
462 xylose forms fucogalactoxyloglucan, which is the main hemicellulose of apple CWs (Aspinall  
463 & Fanous, 1984; Renard, Voragen, Thibault, & Pilnik, 1991). Mannose, the main element of  
464 the hemicellulose mannan (Voragen, Schols, & Pilnik, 1986), increased slightly during apple  
465 fruit storage. Pectins in the AIS of raw apples were highly methylated (> 50 %), in accordance  
466 with previously published values (65-80 %) (Billy et al., 2008; De Vries, Voragen, Rombouts,  
467 & Pilnik, 1981; Le Bourvellec et al., 2011). The DM remained unchanged during storage.  
468 Billy et al. (2008), De Vries, Voragen, Rombouts, and Pilnik (1981) and Gwanpua et al.  
469 (2014) also observe no change in the DM of raw apple CW during post-harvest storage.

470 The AIS content of the pulp (Table 2) was between three to four times higher than AIS of raw  
471 apples. This reflected the concentration of insoluble fibres, namely cellulose, hemicellulose  
472 and insoluble pectins, in the pulp. Major trends of CW composition found in FR were  
473 maintained during apple processing and could be detected in the pulps' polysaccharides. The  
474 main sugar was glucose, coming primarily from cellulose, followed by galacturonic acid. The  
475 starch content was lower than in raw fruit, decreasing to not detectable values at T6. The DM  
476 of pectins occurring in the pulp remained stable over post-harvest storage and was slightly  
477 higher than the DM of raw apple pectins. The sugars constituting the side chains of RG I,  
478 arabinose and galactose, decreased significantly during storage. Sugars associated with

479 hemicelluloses (xylose, mannose and fucose) showed similar or slightly higher values, all  
480 increasing (by balance) during post-harvest storage. Interestingly, AIS of the pulp decreased  
481 significantly over post-harvest storage. However, the pulp wet mass (Fig. 1D) generally  
482 increased. This demonstrated improved water retention capacities of aged cells as calculated  
483 in Table 2, resulting in an alleged higher pulp wet mass. **The water retention capacity of plant  
484 cells is thought to be affected by the porosity of the CW induced by structural changes of CW  
485 polysaccharides and their association (Bidhendi & Geitmann, 2016). Lopez-Sanchez et al.  
486 (2020) showed that calcium cross-linking of HG pectins impedes interaction of pectin chains  
487 with cellulose and thus reduces densification of the CW. As a result, water retention increases.  
488 However, this effect can be excluded in this study: the CW charge, necessary to initiate  
489 calcium cross-linking, did not change over post-harvest storage as the DM of the pectins in  
490 the pulp remained constant. Another study reported an interaction between RG I side chains  
491 and the cellulose-xyloglucan network in the CW (Zykwinska, Ralet, Garnier, & Thibault,  
492 2005). The decreasing amounts of arabinose and galactose during storage (Table 2) might  
493 thus be responsible for CW loosening. Hence, CW porosity could increase and would be able  
494 to retain a higher amount of water.**

495 Serum samples contained low concentrations of soluble polysaccharides, in accordance with  
496 the values (1-5 mg/g FW) found by Le Bourvellec et al. (2011). At T0, the serum AIS  
497 contained high values of glucose and relatively low galacturonic acid. The abnormal values at  
498 T0 could be explained by presence of gelatinized starch in the serum at T0, accounting for  
499 more than half of the AIS. From T1, glucose content was more than five times less and  
500 galacturonic acid became the main sugar. This confirmed that pectins were the main  
501 constituent in serum, as expected (Le Bourvellec et al., 2011). Soluble pectins were highly  
502 methylated and contained arabinose and galactose, probably from RG I side chains, which  
503 decreased significantly until T3. Interestingly, values for arabinose and galactose increased

504 again between three and six months of post-harvest storage. Xylose and fucose, both neutral  
505 sugars deriving from hemicelluloses, showed lower values compared to FR or pulp AIS and  
506 no obvious trend during storage could be observed. No mannose was detected in the serum  
507 AIS. Colin-Henrion, Mehinagic, Renard, Richomme, and Jourjon (2009) and Le Bourvellec et  
508 al. (2011) found similar trends regarding the amount and composition of the AIS in the pulp  
509 and the serum.

510 The CW composition showed a clear decrease of RG I side chains during post-harvest  
511 storage. This might be related to decreasing particle sizes in the puree (see section 3.2.3.) as a  
512 reduction of cell adhesion in apples through RG I debranching has already been described in  
513 literature (Pena & Carpita, 2004). Another study correlated apple fruit softening to a  
514 decreasing number of HG-calcium complexes in the middle lamella (Ng et al., 2013). The  
515 DM of firmer apples should then be less important to initiate cross-linking with calcium ions.  
516 Nevertheless, the latter study showed an increase of firmness without demethylation, leading  
517 to the conclusion that calcium cross-linking does not always induce firmer fruits. As the  
518 calcium content in the fruit is determined at harvest and will not alter significantly during  
519 post-harvest storage (slight changes may only occur due to altered dry matter) and as the  
520 pectins analysed in this study were highly methylated (Table 2), and thus unlikely to form  
521 calcium bridges, these complexes were not considered in this study.

522



523 **Table 2**

524 Yields AIS from fresh weight (mg/g fresh weight), **water retention capacity of the pulp (g/g dry weight)** and compositions (mg/g AIS) of the AIS  
 525 of raw apples (FR), pulp (PL) and serum (SE). Data are averaged from compositions of GS, GD1 and GD2 at a given storage time and puree  
 526 results are those of not refined (NR) samples. For detailed dataset, see Supplementary Table S1.

Storage (months)	Type	Yields AIS	Water retention	Rha	Fuc	Ara	Xyl	Man	Gal	Glc	GalA	MeOH (DM%)	Starch
0	FR	29	10	13	12	138	52	22	127	344	259	34 (70)	220
	PL	103		13	11	130	63	24	135	339	249	36 (80)	72
	SE	3		23	9	96	28	0	122	222	426	73 (92)	554
1	FR	26	11	12	15	125	61	22	93	313	319	40 (70)	54
	PL	89		16	13	130	69	27	101	361	248	36 (81)	27
	SE	2		13	6	71	16	0	79	38	670	107 (86)	176
3	FR	25	12	13	19	106	68	23	74	325	329	44 (74)	5
	PL	87		16	14	106	79	28	84	379	258	35 (76)	4
	SE	1		12	7	55	19	0	55	32	709	111 (89)	12
6	FR	23	13	15	15	95	69	26	74	347	319	41 (73)	2
	PL	76		16	15	101	82	29	84	406	232	36 (86)	0
	SE	2		18	14	69	27	0	64	39	649	120 (100)	9
<i>SD</i>	<i>FR</i>	<i>4</i>	<i>1</i>	<i>3</i>	<i>5</i>	<i>14</i>	<i>6</i>	<i>4</i>	<i>18</i>	<i>31</i>	<i>34</i>	<i>7 (14)</i>	<i>39</i>
	<i>PL</i>	<i>11</i>		<i>2</i>	<i>1</i>	<i>13</i>	<i>5</i>	<i>2</i>	<i>20</i>	<i>24</i>	<i>22</i>	<i>3 (10)</i>	<i>25</i>
	<i>SE</i>	<i>1</i>		<i>3</i>	<i>4</i>	<i>18</i>	<i>10</i>	<i>0</i>	<i>26</i>	<i>135</i>	<i>100</i>	<i>19 (10)</i>	<i>71</i>
<i>Kruskal-Wallis</i>	<i>FR H</i>	<i>7</i>	<i>16</i>	<i>4</i>	<i>6</i>	<i>23</i>	<i>21</i>	<i>11</i>	<i>21</i>	<i>8</i>	<i>15</i>	<i>7 (0.8)</i>	<i>33</i>
	<i>FR P</i>	<i>0.07</i>		<i>0.25</i>	<i>0.10</i>	<b>&lt; 0.05</b>	<b>&lt; 0.05</b>	<b>&lt; 0.05</b>	<b>&lt; 0.05</b>	<i>0.05</i>	<b>&lt; 0.05</b>	<i>0.08 (0.84)</i>	<b>&lt; 0.05</b>
	<i>PL H</i>	<i>16</i>		<i>14</i>	<i>23</i>	<i>18</i>	<i>27</i>	<i>12</i>	<i>18</i>	<i>20</i>	<i>8</i>	<i>0.4 (5)</i>	<i>29</i>

PL P	< 0.05	< 0.05	< 0.05	< 0.05	< 0.05	< 0.05	< 0.05	< 0.05	< 0.05	< 0.05	0.05	0.94 (0.21)	< 0.05
SE H	10		25	15	18	9	-	27	3	23		14 (9)	30
SE P	< 0.05		< 0.05	< 0.05	< 0.05	< 0.05	-	< 0.05	0.34	< 0.05		< 0.05 (<0.05)	< 0.05

527 Rha: Rhamnose; Fuc: Fucose; Ara: Arabinose; Xyl: Xylose; Man: Mannose; Gal: Galactose; Glc: Glucose without starch; GalA: Galacturonic

528 acid; MeOH: Methanol; DM%: Degree of methylation; SD: Standard deviation of the mean (degrees of freedom: 32). All values were corrected

529 for the starch content. Yields of AIS in serum and pulp are expressed relative to the weight of serum and pulp, respectively, collected after

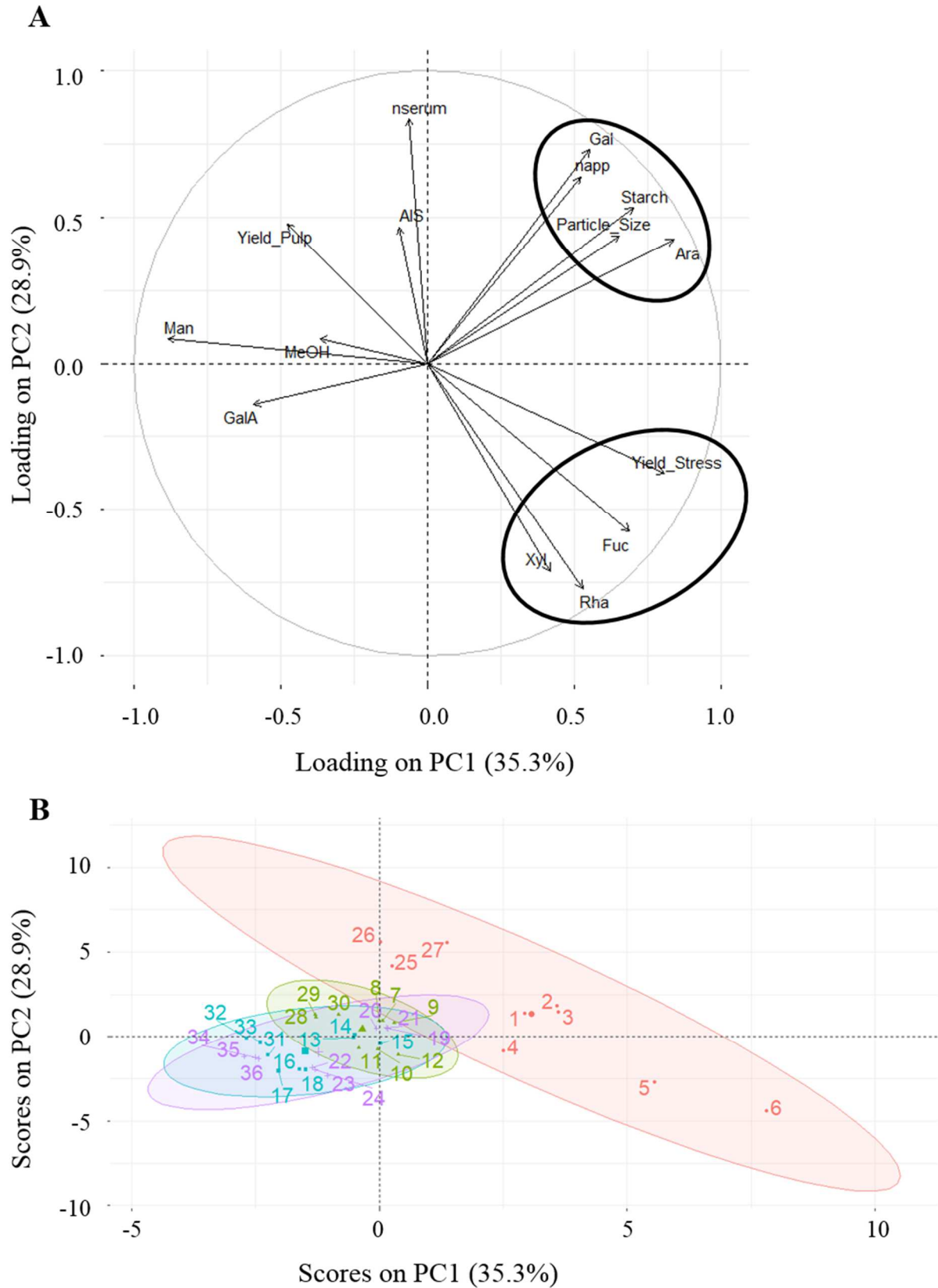
530 centrifugation.

531 *3.4. Relationship between pectin composition and the purees' texture*

532

533 In order to visualize the relation between the puree's viscosity, its determining factors (CW  
534 content, particle size, serum viscosity) and pectin composition of the puree, a principal  
535 component analysis (PCA) was performed (Fig. 3). The first two principal components (PC1  
536 and PC2) explained together nearly 65 % of the total variance. A group of correlated variables  
537 (Fig. 3A) was that comprising puree's viscosity (napp), starch content in the puree (Starch,  
538 deduced from starch analysis of raw apples), particle size (Particle\_Size) and the pectic sugars  
539 arabinose (Ara) and galactose (Gal). All these parameters decreased during post-harvest  
540 storage and allowed differentiation of the purees by post-harvest storage duration (Fig. 3B).  
541 *Although the studied apple cultivars and agricultural practices showed significant differences*  
542 *for both textural characteristics and pectin composition (Supplementary Table S1), their CW*  
543 *structure failed to explain puree's texture. It was thus decided to not further consider these*  
544 *parameters and to group the samples by post-harvest storage.* "Starch" was most modified  
545 between T0 and T1, which could be linked with individuation of the T0 samples on the  
546 sample map. Mannose (Man) contributed highly to PC1, which was probably linked to the  
547 higher mannose content in GS apples (Supplementary Table S1), as all GS samples were  
548 shifted to the negative side of PC1 relative to GD. Serum viscosity (nserum) was highly  
549 accounted for on PC2 (Fig. 3A). A second group of correlated variables was that of xylose  
550 (Xyl), fucose (Fuc) (both key components of fucogalactoxyloglucans), rhamnose (Rha) and to  
551 a lesser extent yield stress (Yield\_Stress). Puree's AIS (AIS), methanol (MeOH), galacturonic  
552 acid content (GalA) and pulp wet mass (Yield\_Pulp) were all poorly represented on plane  
553 1x2. Interestingly, purees at T0 showed a high dispersion, whereas the other purees were less  
554 dispersed. According to these results, puree's viscosity was mainly affected by starch content  
555 and particle size, both parameters that decreased during post-harvest storage of apples.

556 In model systems, the apple puree's texture was shown to be determined by the volume  
557 occupied by the particles, that is to say their quantity and size (Espinosa-Munoz, Renard,  
558 Symoneaux, Biau, & Cuvelier, 2013; Leverrier, Almeida, Espinosa-Munoz, & Cuvelier,  
559 2016). In these reconstituted systems, the amount of insoluble cell walls (AIS) and the size of  
560 the particles could be varied independently, so that the insoluble solids content has a first-  
561 order effect on the rheological behaviour of apple purees. In real systems, however, particle  
562 size seemed to be the most important factor determining the puree's texture, given the fact  
563 that the amount of AIS did not change sufficiently to have an impact on texture.



564

565 **Fig. 3.** Principal component analysis (PCA) of neutral sugars, rheological and structural  
 566 characteristics of apple purees over post-harvest storage. Correlation circle of variables

567 loadings on PC1 (33.8 %) and PC2 (27.4 %) (A). Sample map of scores on PC1 (33.8 %) and  
568 PC2 (27.4 %) as function of post-harvest storage (B). The red ellipse represents samples at  
569 T0, the green ellipse samples at T1, the blue ellipse samples at T3 and the violet ellipse  
570 samples at T6. All correlation ellipses correspond to the 95 % confidence interval around the  
571 barycentre. Only not refined (NR) samples were considered and the values of AIS and neutral  
572 sugars were corrected for the starch content (deduced from starch analysis of raw apples).  
573 napp: Apparent viscosity of the puree at 50 s<sup>-1</sup>; Yield\_Stress: Yield stress of the puree;  
574 nserum: Serum viscosity at 100 s<sup>-1</sup>; Yield\_Pulp: Pulp wet mass; Particle\_Size: Particle size in  
575 the puree (d 0.9); AIS: Alcohol Insoluble Solids; Rha: Rhamnose; Fuc: Fucose; Ara:  
576 Arabinose; Xyl: Xylose; Man: Mannose; Gal: Galactose; GalA: Galacturonic acid; MeOH:  
577 Methanol; Starch: Starch in the puree (deduced from starch analysis of raw apples). 1-3:  
578 T0\_GD1; 4-6: T0\_GD2; 7-9: T1\_GD1; 10-12: T1\_GD2; 13-15: T3\_GD1; 16-18: T3\_GD2;  
579 19-21: T6\_GD1; 22-24: T6\_GD2; 25-27: T0\_GS; 28-30: T1\_GS; 31-33: T3\_GS; 34-36:  
580 T6\_GS (GD1: Golden Delicious, reduced fruit load; GD2: Golden Delicious, high fruit load;  
581 GS: Granny Smith; T0: Directly after harvest; T1: After 1 month of post-harvest storage;  
582 T3: After 3 months of post-harvest storage; T6: After 6 months of post-harvest storage).

583

### 584 *3.5. Macromolecular characteristics of soluble pectins*

585

586 The decrease of particle size over post-harvest storage could be further explained by analysis  
587 of the macromolecular characteristics of soluble pectins. As they followed common trends  
588 over post-harvest storage and processing, they were averaged from the samples of GD1, GD2  
589 and GS (Table 3). Although the structural features of soluble pectins varied according to  
590 different cultivars and agricultural practices (Supplementary Table S2), no clear trend could  
591 be detected.

592 GD2 was chosen as a representative example to illustrate the molar mass distribution of  
593 soluble pectins in raw apples (Fig. 4A) and sera (Fig. 4B). Both showed a shift of the main  
594 peak to higher elution volumes, i.e. polysaccharides of smaller macromolecular sizes, during  
595 storage. This shift was the most drastic during the first month of post-harvest storage. A  
596 second, narrower peak was detected at high elution volumes. Interestingly, its concentration  
597 diminished from T0 to T6. However, starch could be excluded to contribute to this peak as the  
598 determined molar mass was too small compared to values reported in literature ( $1.0 \times 10^8$ –  
599  $4.8 \times 10^8$  g/mol) (Rolland-Sabate, Guilois, Jaillais, & Colonna, 2011). Hence, this peak was  
600 assigned to some oligosaccharides remaining in the AIS. Molar mass of soluble pectins  
601 (Table 3) in raw apples decreased significantly during post-harvest storage. The viscometric  
602 hydrodynamic radius also decreased for raw apple pectins, further confirming a decrease in  
603 pectin size during apple storage. Gwanpua et al. (2014) also showed a decrease in molar mass  
604 of water soluble pectins during post-harvest storage of apples and ascribed this change to  
605 either pectin depolymerisation, an extensive loss of RG I side chains or both. Molar mass of  
606 serum pectins only decreased during the first month of post-harvest storage, before a slight  
607 increase was observed at T6. The same trend was observed for the hydrodynamic radius.  
608 Apparently, high molar mass pectins could be extracted during puree processing at T6.

609 During the first month of post-harvest storage,  $[\overline{\eta}]_z$  of both raw apple and serum pectins  
610 increased even if molar mass decreased (Table 3). This was due to structural changes in  
611 soluble pectins, showing more extended and less dense conformations during storage.  
612 However,  $[\overline{\eta}]_z$  decreased for raw apples and sera at T6 while molar mass values kept  
613 decreasing (raw fruit pectins) or remained similar (serum pectins). This indicated presence of  
614 pectins with less extended and denser conformations. The shape and structure of  
615 polysaccharides can also be assessed by calculating the  $\rho$ -parameter ( $\rho = \overline{R}_{gz}/\overline{R}_{hz}$ ) which has  
616 theoretical values of  $\sim 1.0$  for soft spheres, values higher than 1.5 for linear polymers and

617 increasing values with the linearity and the stiffness of the system (Burchard, 1983). This  
618 ratio increased for soluble pectins of raw apples over post-harvest storage, indicating a  
619 process of shape extension of soluble raw apple pectins that corresponds well to the  
620 linearization of the pectins. In contrast, the  $\rho$ -parameter increased for serum pectins until T1,  
621 then decreased slightly. Thus, serum pectins seemed to be the most linear at T1.

622 In summary, macromolecular sizes and molar masses of raw apple pectins decreased during  
623 prolonged post-harvest storage. In addition, they became more linear, probably due to RG I  
624 side chain hydrolysis. The decrease of neutral sugars arabinose and galactose during storage,  
625 as detected in section 3.3., supported this hypothesis. Serum pectins revealed the same trend  
626 during the first month of post-harvest storage. At T6, in contrast, high molar mass pectins  
627 could be extracted during puree processing. They also showed less linear characteristics, in  
628 line with increased arabinose and galactose contents of serum pectins at T6 (section 3.3.).

629 RG I side chains were found to interact with the cellulose-xyloglucan network in the CW  
630 (Zykwinska, Ralet, Garnier, & Thibault, 2005). We thus think that RG I side chain hydrolysis  
631 as well as a decrease in macromolecular size and molar mass of raw apple pectins during  
632 storage reduced pectin entanglement in the CW structure. This might enhance extractability of  
633 high molar mass pectins from RG I regions during processing.

634 Interestingly, soluble pectins in raw apples and sera showed the same macromolecular size  
635 but different molar masses both at T0 (Fig. 5A) and T6 (Fig. 5B). At T0 and T1, soluble  
636 pectins in raw fruits showed higher molar masses than serum pectins (Table 3). Processing at  
637 T0 and T1 did thus not lead to degradation of the pectic main chain (same macromolecular  
638 size) but to loss of RG I side chains (decreased molar mass). In addition, serum pectins  
639 exhibited similar  $\bar{R}_{hz}(v)$  but higher  $[\bar{\eta}]_z$  and  $\rho$  values at T0 and T1, further confirming  
640 existence of more linear and thus less branched pectins in the serum. However, at T6, serum  
641 pectins showed higher molar masses, higher  $\bar{R}_{hz}(v)$  and  $[\bar{\eta}]_z$  but lower  $\rho$  values at same



642 macromolecular sizes compared to raw fruit pectins. It thus seemed that, after prolonged post-  
 643 harvest storage, less linear and more branched pectins could be solubilized in the serum,  
 644 probably because they were less attached to the CW. However, no simple links were found  
 645 between serum viscosity and the molar mass of soluble pectins.

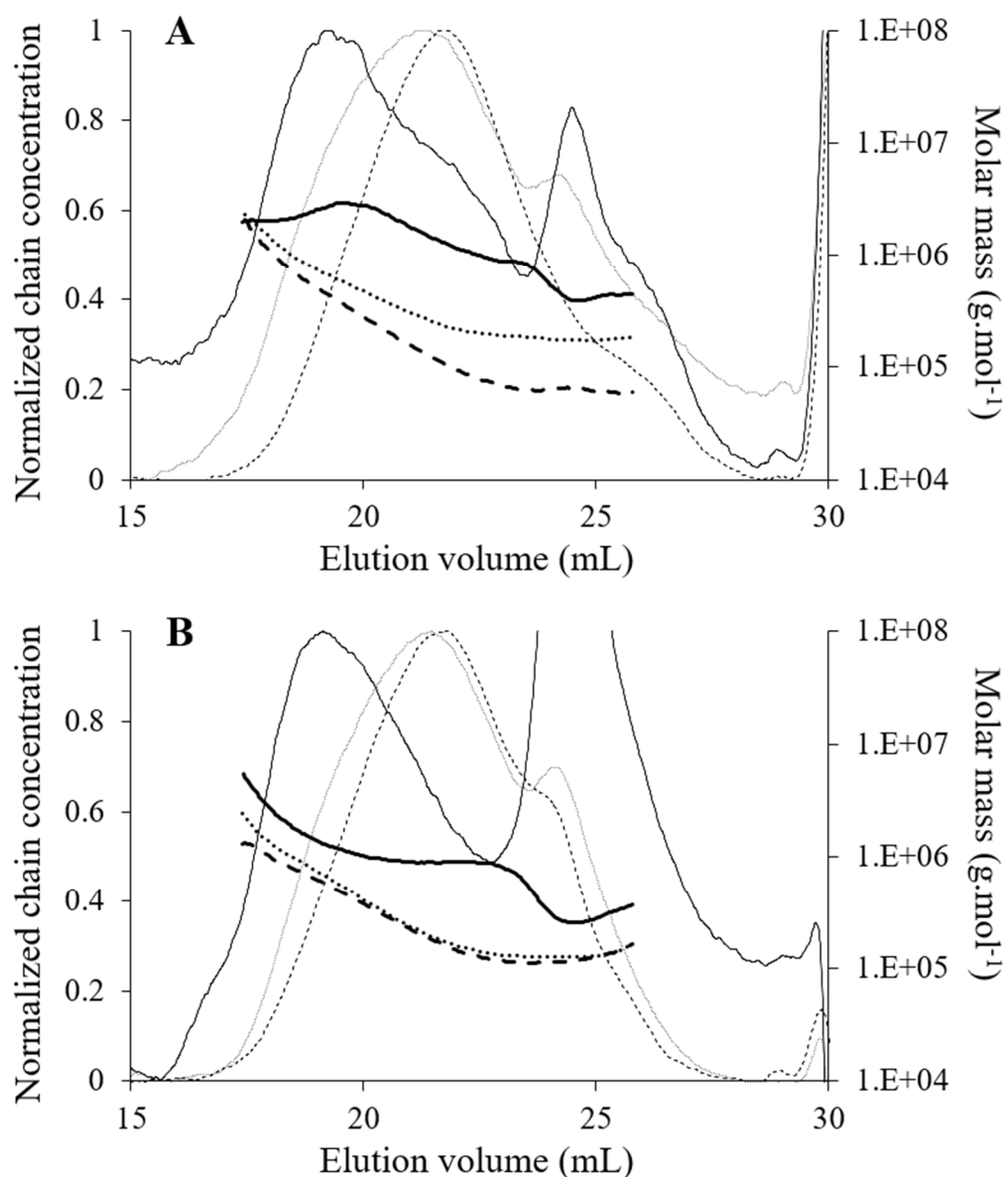
646

647 **Table 3**

648 Evolution of macromolecular features of soluble pectins in raw apples (FR) and  
 649 corresponding sera (SE) during post-harvest storage measured by HPSEC-MALLS coupled to  
 650 online viscometry. Data are averaged from compositions of GS, GD1 and GD2 at a given  
 651 storage time and serum results are those of not refined (NR) samples. For detailed dataset, see  
 652 Supplementary Table S2.

Storage (months)	Type	$\bar{M}_w \times 10^3$ (g/mol)	$\bar{R}_{hz}(v)$ (nm)	$[\eta]_z$ (mL/g)	$\rho = \bar{R}_{gz}/\bar{R}_{hz}(v)$
0	FR	1374	66	1162	0.9
	SE	924	68	1619	1.0
1	FR	430	50	1496	1.3
	SE	361	51	1721	1.5
6	FR	181	40	1396	1.6
	SE	410	52	1502	1.4
<i>SD</i>	<i>FR</i>	<i>215</i>	<i>5</i>	<i>210</i>	<i>0.1</i>
	<i>SE</i>	<i>157</i>	<i>8</i>	<i>212</i>	<i>0.2</i>
<i>Kruskal-Wallis</i>	<i>FR H</i>	<i>23</i>	<i>16</i>	<i>11</i>	<i>21</i>
	<i>FR P</i>	<b>&lt;0.05</b>	<b>&lt;0.05</b>	<b>&lt;0.05</b>	<b>&lt;0.05</b>
	<i>SE H</i>	<i>17</i>	<i>8</i>	<i>4</i>	<i>14</i>
	<i>SE P</i>	<b>&lt;0.05</b>	<b>&lt;0.05</b>	<i>0.17</i>	<b>&lt;0.05</b>

653 FR: Raw fruit; SE: Serum;  $\bar{M}_w$ : weight-average molar mass;  $\bar{R}_{hz}(v)$ : z-average viscometric  
 654 hydrodynamic radius;  $[\eta]_z$ : z-average intrinsic viscosity;  $\bar{R}_{gz}$ : z-average radius of gyration;  
 655 SD: Standard deviation of the mean (degrees of freedom: 22).



656

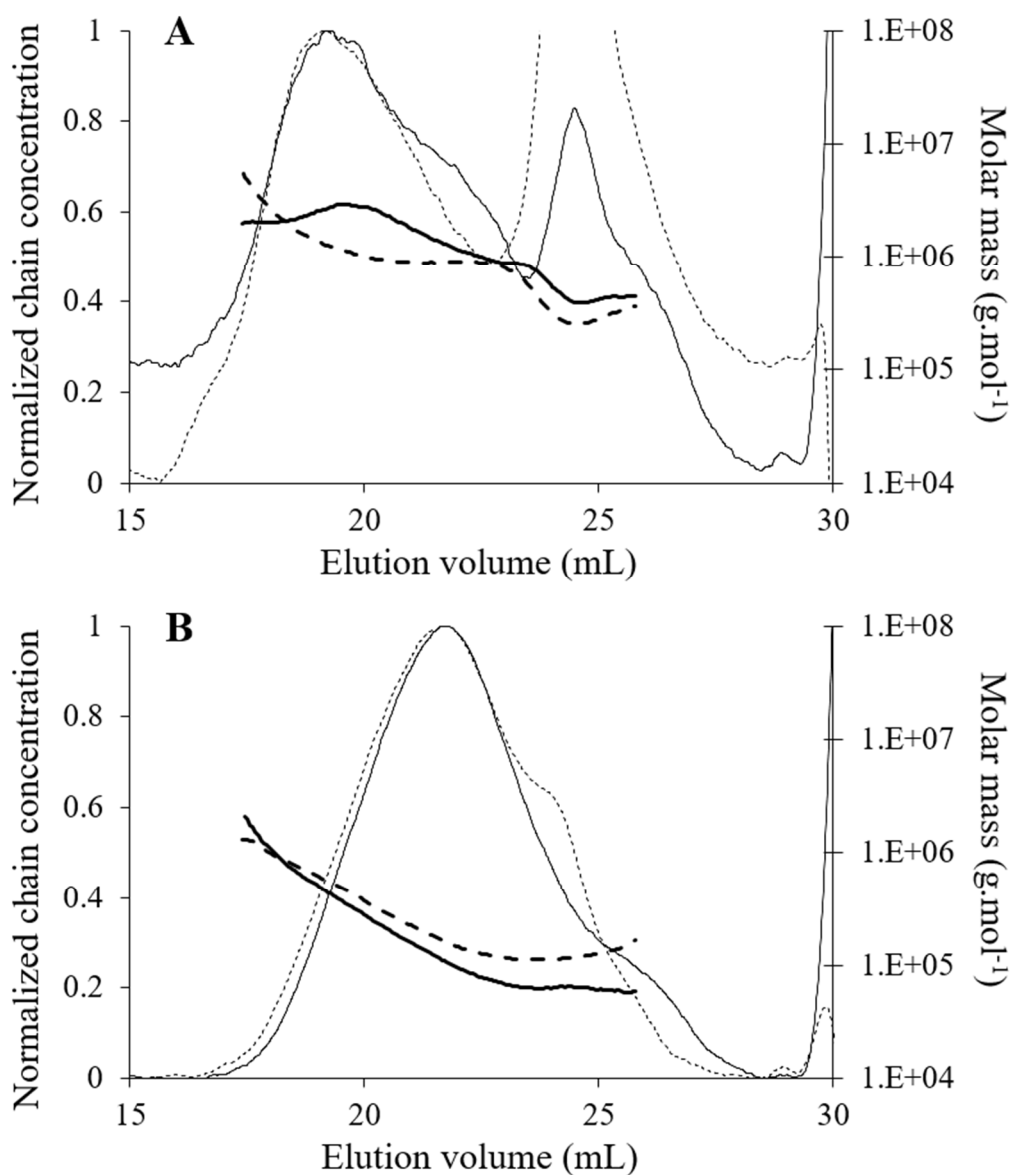
657 **Fig. 4.** Representative chromatograms for the cultivar GD2 in the function of storage.

658 Normalized chain concentration and molar mass versus elution volume of soluble pectins in

659 raw apples (A) and sera (B). Continuous lines represent samples at T0, dotted lines samples at

660 T1 and dashed lines samples at T6. The signal (mV) obtained by the RID detector was

661 normalised through dividing all data points by the peak signal.



662

663 **Fig. 5.** Representative chromatograms for the cultivar GD2 in the function of the type (raw  
 664 apple versus serum pectins). Normalized chain concentration and molar mass versus elution  
 665 volume of soluble pectins at T0 (A) and T6 (B). Continuous lines represent raw apple and  
 666 dashed lines serum pectins. The signal (mV) obtained by the RID detector was normalised  
 667 through dividing all data points by the peak signal.

668

669

670

671 **4. Conclusions**

672

673 Post-harvest storage duration influenced puree's viscosity the most, whereas the CW  
674 composition of apple cultivars and agricultural practices failed to explain the puree's texture.  
675 However, they all showed similar trends during storage. Particle size decreased during  
676 prolonged post-harvest storage and seemed to be the most important factor determining  
677 puree's texture as smaller particles generated less viscous purees. When two purees showed  
678 similar particle sizes, pulp wet mass determined texture. In raw apples, prolonged storage led  
679 to pectin RG I side chain hydrolysis as well as to a reduction of soluble pectins'  
680 macromolecular size and molar mass. This promoted softening of apple tissue due to reduced  
681 cell adhesion, leading to facilitated fragmentation during processing. In addition, water  
682 retention capacities of the cells increased when aged, probably due to elevated porosity as the  
683 pectins were less entangled in the CW structure. During puree processing, prolonged post-  
684 harvest storage facilitated extractability of high molar mass pectins that were less linear and  
685 more branched. However, the pectic main chain was not degraded during processing.

686

687 **CRedit authorship contribution statement**

688

689 **Alexandra Buergy:** Investigation, Formal analysis, Data curation, Writing - original draft.

690 **Agnès Rolland-Sabaté:** Supervision, Validation, Writing - review & editing. **Alexandre**

691 **Leca:** Investigation, Supervision, Writing - review & editing. **Catherine M. G. C. Renard:**

692 Conceptualization, Funding acquisition, Project administration, Validation, Writing - review

693 & editing.

694

695

696 **Declaration of competing interest**

697

698 Declarations of interest: none.

699

700 **Acknowledgements**

701

702 This work was carried out as part of “Interfaces” flagship project, publicly funded through  
703 ANR (the French National Agency) under the “Investissements d’avenir” program with the  
704 reference ANR-10-LABX-001-01 Labex Agro and coordinated by Agropolis Fondation under  
705 the reference ID 1603-001.

706

707 **Appendix A. Supplementary data**

708

709 Supplementary Table S1

710 Supplementary Table S2

711

712 **References**

713

714 Albersheim, P., Darvill, A. G., O’Neill, M. A., Schols, H. A., & Voragen, A. G. J. (1996). An  
715 hypothesis: The same six polysaccharides are components of the primary cell walls of  
716 all higher plants. In J. Visser & A. G. J. Voragen (Eds.), *Pectins and Pectinases* (Vol.  
717 14, pp. 47-55). Amsterdam: Elsevier Science BV.

718 **Aspinall, G. O., & Fanous, H. K. (1984). Structural investigations on the non-starchy**  
719 **polysaccharides of apples. *Carbohydrate Polymers*, 4(3), 193-214.**

720 Bidhendi, A. J., & Geitmann, A. (2016). Relating the mechanics of the primary plant cell wall  
721 to morphogenesis. *Journal of Experimental Botany*, 67(2), 449-461.

722 Billy, L., Mehinagic, E., Royer, G., Renard, C., Arvisenet, G., Prost, C., & Jourjon, F. (2008).  
723 Relationship between texture and pectin composition of two apple cultivars during  
724 storage. *Postharvest Biology and Technology*, 47(3), 315-324.

725 Blumenkrantz, N., & Asboe-Hansen, G. (1973). New method for quantitative-determination  
726 of uronic acids. *Analytical Biochemistry*, 54(2), 484-489.

727 Box, G. E. P., Hunter, W. G., & Hunter, J. S. (1978). *Statistics for Experimenters: An*  
728 *Introduction to Design, Data Analysis, and Model Building*. New York: John Wiley  
729 and Sons.

730 Burchard, W. (1983). Static and dynamic light scattering from branched polymers and  
731 biopolymers. In *Light Scattering from Polymers. Advances in Polymer Science* (Vol.  
732 48, pp. 1-124). Berlin, Heidelberg: Springer Berlin Heidelberg.

733 Carpita, N. C., & Gibeaut, D. M. (1993). Structural models of primary-cell walls in flowering  
734 plants - Consistency of molecular-structure with the physical-properties of the walls  
735 during growth. *Plant Journal*, 3(1), 1-30.

736 Colin-Henrion, M., Mehinagic, E., Renard, C. M. G. C., Richomme, P., & Jourjon, F. (2009).  
737 From apple to apple sauce: Processing effects on dietary fibres and cell wall  
738 polysaccharides. *Food Chemistry*, 117(2), 254-260.

739 Darvill, A.G., McNeil, M., Albersheim, P., & Delmer, D.P. (1980). The plant cell. In P.K.  
740 Stumpf, & E.E. Conn (Eds.), *The biochemistry of plants* (Vol. 1, pp. 91-162). New  
741 York: Academic Press.

742 De Vries, J. A., Voragen, A. G. J., Rombouts, F. M., & Pilnik, W. (1981). Extraction and  
743 purification of pectins from Alcohol Insoluble Solids from ripe and unripe apples.  
744 *Carbohydrate Polymers*, 1(2), 117-127.

745 Dubois, M., Gilles, K. A., Hamilton, J. K., Rebers, P. A., & Smith, F. (1956). Colorimetric  
746 method for determination of sugars and related substances. *Analytical Chemistry*,  
747 28(3), 350-356.

748 Einstein, A. (1906). Eine neue Bestimmung der Moleküldimensionen. *Annalen der Physik*,  
749 324(2), 289-306.

750 Einstein, A. (1911). Berichtigung zu meiner Arbeit: „Eine neue Bestimmung der  
751 Moleküldimensionen“. *Annalen der Physik*, 339(3), 591-592.

752 Englyst, H., Wiggins, H. S., & Cummings, J. H. (1982). Determination of the non-starch  
753 polysaccharides in plant-foods by gas-liquid-chromatography of constituent sugars as  
754 alditol acetates. *Analyst*, 107(1272), 307-318.

755 Espinosa-Munoz, L., Renard, C., Symoneaux, R., Biau, N., & Cuvelier, G. (2013). Structural  
756 parameters that determine the rheological properties of apple puree. *Journal of Food*  
757 *Engineering*, 119(3), 619-626.

758 Espinosa, L., To, N., Symoneaux, R., Renard, C., Biau, N., & Cuvelier, G. (2011). Effect of  
759 processing on rheological, structural and sensory properties of apple puree. In G.  
760 Saravacos, P. Taoukis, M. Krokida, V. Karathanos, H. Lazarides, N. Stoforos, C. Tzia  
761 & S. Yanniotis (Eds.), *11th International Congress on Engineering and Food* (Vol. 1,  
762 pp. 513-520). Amsterdam: Elsevier Science BV.

763 Fischer, M., & Amado, R. (1994). Changes in the pectic substances of apples during  
764 development and postharvest ripening. Part 1: Analysis of the alcohol insoluble  
765 residue. *Carbohydrate Polymers*, 25(3), 161-166.

766 Goffinet, M. C., Robinson, T. L., & Lakso, A. N. (1995). A comparison of ‘Empire’ apple  
767 fruit size and anatomy in unthinned and hand-thinned trees. *Journal of Horticultural*  
768 *Science*, 70(3), 375-387.

769 Gross, K. C., & Sams, C. E. (1984). Changes in cell wall neutral sugar composition during  
770 fruit ripening: a species survey. *Phytochemistry*, 23(11), 2457-2461.

771 Guillemain, F., Guillon, F., Bonnin, E., Devaux, M. F., Chevalier, T., Knox, J. P., Liners, F., &  
772 Thibault, J. F. (2005). Distribution of pectic epitopes in cell walls of the sugar beet  
773 root. *Planta*, 222(2), 355-371.

774 Gwanpua, S. G., Van Buggenhout, S., Verlinden, B. E., Christiaens, S., Shpigelman, A.,  
775 Vicent, V., Kermani, Z. J., Nicolai, B. M., Hendrickx, M., & Geeraerd, A. (2014).  
776 Pectin modifications and the role of pectin-degrading enzymes during postharvest  
777 softening of Jonagold apples. *Food Chemistry*, 158, 283-291.

778 Khan, A. A., & Vincent, J. F. V. (1990). Anisotropy of apple parenchyma. *Journal of the*  
779 *Science of Food and Agriculture*, 52(4), 455-466.

780 Kohn, R., & Luknár, O. (1977). Intermolecular calcium ion binding on polyuronates-  
781 polygalacturonate and polyguluronate. *Collection of Czechoslovak Chemical*  
782 *Communications*, 42, 731-744.

783 Koziol, A., Cybulska, J., Pieczywek, P. M., & Zdunek, A. (2017). Changes of pectin  
784 nanostructure and cell wall stiffness induced in vitro by pectinase. *Carbohydrate*  
785 *Polymers*, 161, 197-207.

786 Kruskal, W. H., & Wallis, W. A. (1952). Use of Ranks in One-Criterion Variance Analysis.  
787 *Journal of the American Statistical Association*, 47(260), 583-621.

788 Lan, W., Jaillais, B., Leca, A., Renard, C. M. G. C., & Bureau, S. (2020). A new application  
789 of NIR spectroscopy to describe and predict purees quality from the non-destructive  
790 apple measurements. *Food Chemistry*, 310, 125944.

791 Le Bourvellec, C., Bouzerzour, K., Ginies, C., Regis, S., Ple, Y., & Renard, C. M. G. C.  
792 (2011). Phenolic and polysaccharidic composition of applesauce is close to that of  
793 apple flesh. *Journal of Food Composition and Analysis*, 24(4-5), 537-547.



794 Lê, S., Josse, J., & Husson, F. (2008). FactoMineR: An R Package for Multivariate Analysis.  
795 *Journal of Statistical Software*, 25(1), 1-18.

796 Leverrier, C., Almeida, G., Espinosa-Munoz, L., & Cuvelier, G. (2016). Influence of Particle  
797 Size and Concentration on Rheological Behaviour of Reconstituted Apple Purees.  
798 *Food Biophysics*, 11(3), 235-247.

799 Leverrier, C., Moulin, G., Cuvelier, G., & Almeida, G. (2017). Assessment of deformability  
800 of soft plant cells by 3D imaging. *Food Structure*, 14, 95-103.

801 Lopez-Sanchez, P., Martinez-Sanz, M., Bonilla, M. R., Sonni, F., Gilbert, E. P., & Gidley, M.  
802 J. (2020). Nanostructure and poroviscoelasticity in cell wall materials from onion,  
803 carrot and apple: Roles of pectin. *Food Hydrocolloids*, 98, 105253.

804 Market Research Future (2019). Fruit Puree Market Research Report- Forecast to 2023.  
805 <https://www.marketresearchfuture.com/reports/fruit-puree-market-5281/> Accessed 15  
806 January 2020.

807 Massiot, P., & Renard, C. (1997). Composition, physico-chemical properties and enzymatic  
808 degradation of fibres prepared from different tissues of apple. *Food Science and*  
809 *Technology – Lebensmittel-Wissenschaft & Technologie*, 30(8), 800-806.

810 Milić, B., Tarlanović, J., Keserović, Z., Zorić, L., Blagojević, B., & Magazin, N. (2017). The  
811 Growth of Apple Central Fruits as Affected by Thinning with NAA, BA and  
812 Naphthenic Acids. *Erwerbs-Obstbau*, 59(3), 185-193.

813 Mohnen, D. (2008). Pectin structure and biosynthesis. *Current Opinion in Plant Biology*,  
814 11(3), 266-277.

815 Ng, J. K. T., Schroder, R., Sutherland, P. W., Hallett, I. C., Hall, M. I., Prakash, R., Smith, B.  
816 G., Melton, L. D., & Johnston, J. W. (2013). Cell wall structures leading to cultivar  
817 differences in softening rates develop early during apple (*Malus x domestica*) fruit  
818 growth. *BMC Plant Biology*, 13.

819 O'Neill, M. A., Warrenfeltz, D., Kates, K., Pellerin, P., Doco, T., Darvill, A. G., &  
820 Albersheim, P. (1996). Rhamnogalacturonan-II, a pectic polysaccharide in the walls of  
821 growing plant cell, forms a dimer that is covalently cross-linked by a borate ester - In  
822 vitro conditions for the formation and hydrolysis of the dimer. *Journal of Biological*  
823 *Chemistry*, 271(37), 22923-22930.

824 Pena, M. J., & Carpita, N. C. (2004). Loss of highly branched arabinans and debranching of  
825 rhamnogalacturonan I accompany loss of firm texture and cell separation during  
826 prolonged storage of apple. *Plant Physiology*, 135(3), 1305-1313.

827 R Core Team (2018). R: A language and environment for statistical computing. R Foundation  
828 for Statistical Computing, Vienna, Austria. <https://www.R-project.org/> Accessed 14  
829 March 2018.

830 Rao, M. A. (1992). The structural approach to rheology of plant food dispersions. *Revista*  
831 *Espanola De Ciencia Y Tecnologia De Alimentos*, 32(1), 3-17.

832 Rao, M. A., Cooley, H. J., Nogueira, J. N., & McLellan, M. R. (1986). Rheology of apple  
833 sauce - effect of apple cultivar, firmness, and processing parameters. *Journal of Food*  
834 *Science*, 51(1), 176-179.

835 Renard, C. M. G. C. (2005). Variability in cell wall preparations: quantification and  
836 comparison of common methods. *Carbohydrate Polymers*, 60(4), 515-522.

837 Renard, C. M. G. C., & Ginies, C. (2009). Comparison of the cell wall composition for flesh  
838 and skin from five different plums. *Food Chemistry*, 114(3), 1042-1049.

839 Renard, C. M. G. C., Voragen, A. G. J., Thibault, J. F., & Pilnik, W. (1991). Studies on apple  
840 protopectin. IV: Apple xyloglucans and influence of pectin extraction treatments on  
841 their solubility. *Carbohydrate Polymers*, 15(4), 387-403.

842 Ridley, B. L., O'Neill, M. A., & Mohnen, D. A. (2001). Pectins: structure, biosynthesis, and  
843 oligogalacturonide-related signaling. *Phytochemistry*, 57(6), 929-967.

844 Robertson, J. A., de Monredon, F. D., Dysseler, P., Guillon, F., Amado, R., & Thibault, J.-F.  
845 (2000). Hydration properties of dietary fibre and resistant starch: a European  
846 collaborative study. *Food Science and Technology – Lebensmittel-Wissenschaft &*  
847 *Technologie*, 33(2), 72-79.

848 Rolland-Sabaté, A., Colonna, P., Potocki-Véronèse, G., Monsan, P., & Planchot, V. (2004).  
849 Elongation and insolubilisation of  $\alpha$ -glucans by the action of *Neisseria polysaccharea*  
850 amylosucrase. *Journal of Cereal Science*, 40(1), 17–30.

851 Rolland-Sabate, A., Guilois, S., Jaillais, B., & Colonna, P. (2011). Molecular size and mass  
852 distributions of native starches using complementary separation methods:  
853 Asymmetrical Flow Field Flow Fractionation (A4F) and Hydrodynamic and Size  
854 Exclusion Chromatography (HDC-SEC). *Analytical and Bioanalytical Chemistry*,  
855 399(4), 1493-1505.

856 Saeman, J. F., Moore, W. E., Mitchell, R. L., & Millett, M. A. (1954). Techniques for the  
857 determination of pulp constituents by quantitative paper chromatography. *Tappi*,  
858 37(8), 336-343.

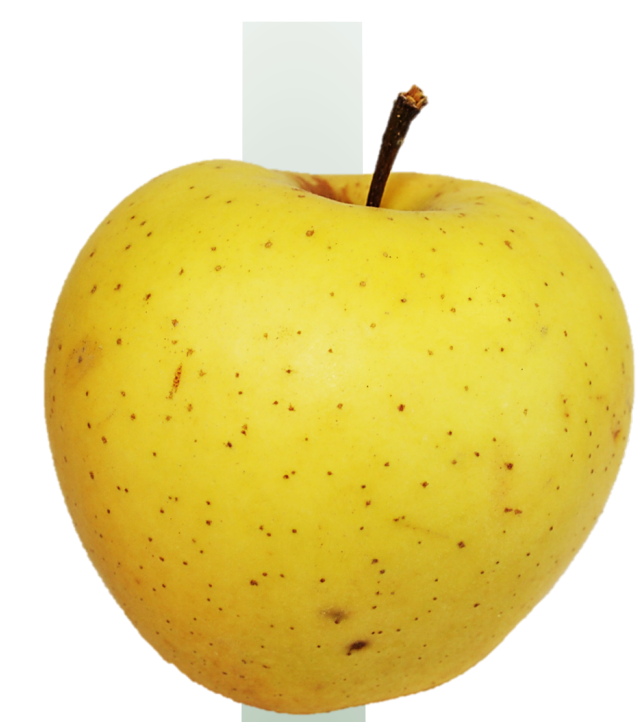
859 Schijvens, E. P. H. M., van Vliet, T., & van Dijk, C. (1998). Effect of processing conditions  
860 on the composition and rheological properties of applesauce. *Journal of Texture*  
861 *Studies*, 29(2), 123-143.

862 Simha, R. (1940). The influence of Brownian movement on the viscosity of solutions. *The*  
863 *Journal of Physical Chemistry*, 44(1), 25-34.

864 Stokes, J. R. (2012). ‘Oral’ Rheology. In J. Chen, & L. Engelen (Eds.), *Food Oral*  
865 *Processing: Fundamentals of eating and sensory perception* (pp. 227-264). Wiley-  
866 Blackwell.

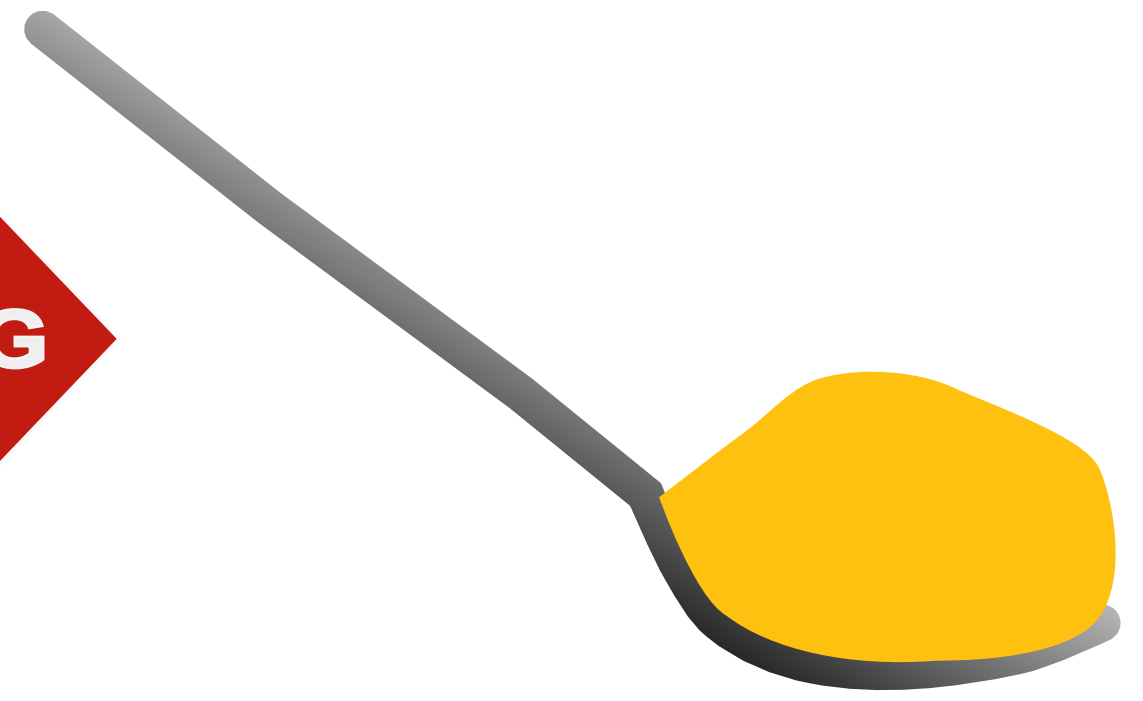
867 Thakur, B. R., Singh, R. K., & Handa, A. K. (1997). Chemistry and uses of pectin - A review.  
868 *Critical Reviews in Food Science and Nutrition*, 37(1), 47-73.

- 869 Voragen, F. G. J., Schols, H. A., & Pilnik, W. (1986). Structural features of the hemicellulose  
870 polymers of apples. *Zeitschrift für Lebensmittel-Untersuchung und Forschung*, 183(2),  
871 105-110.
- 872 Waldron, K. W., Smith, A. C., Parr, A. J., Ng, A., & Parker, M. L. (1997). New approaches to  
873 understanding and controlling cell separation in relation to fruit and vegetable texture.  
874 *Trends in Food Science & Technology*, 8(7), 213-221.
- 875 Wismer, P. T., Proctor, J. T. A., & Elfving, D. C. (1995). Benzyladenine Affects Cell  
876 Division and Cell Size during Apple Fruit Thinning. *Journal of the American Society  
877 for Horticultural Science*, 120(5), 802.
- 878 Zykwinska, A. W., Ralet, M. C., Garnier, C. D., & Thibault, J. F. (2005). Evidence for in  
879 vitro binding of pectin side chains to cellulose. *Plant Physiology*, 139(1), 397-407.

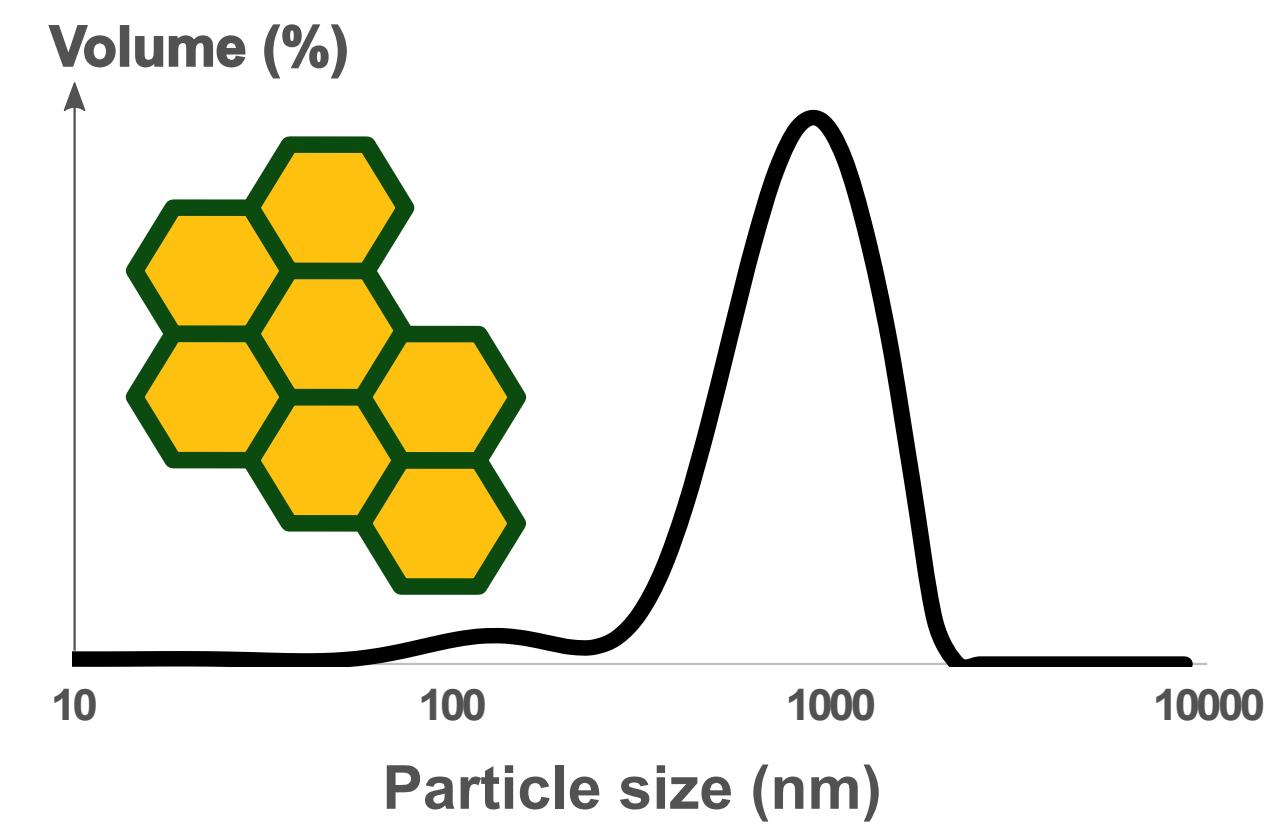


**At Harvest**

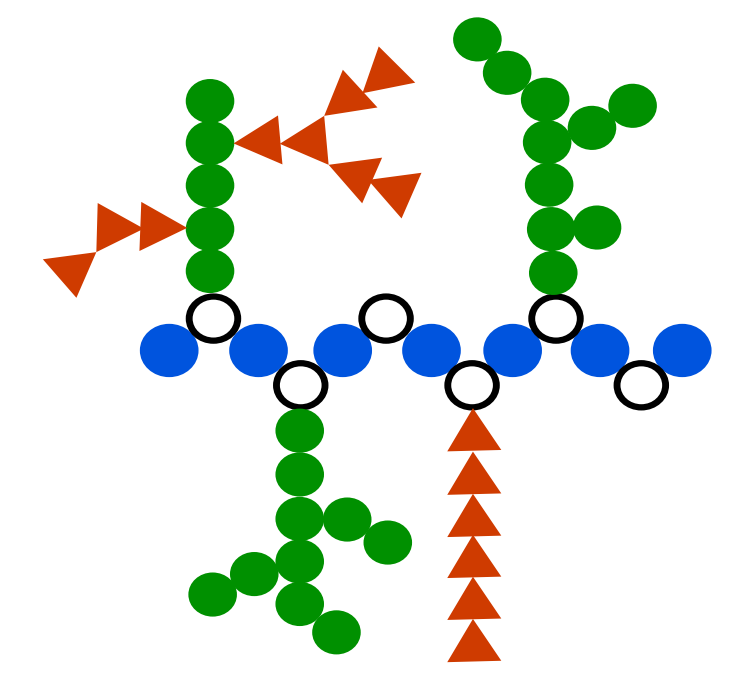
**PROCESSING**



**High viscosity  
of the apple puree**



**Large cell fragments**

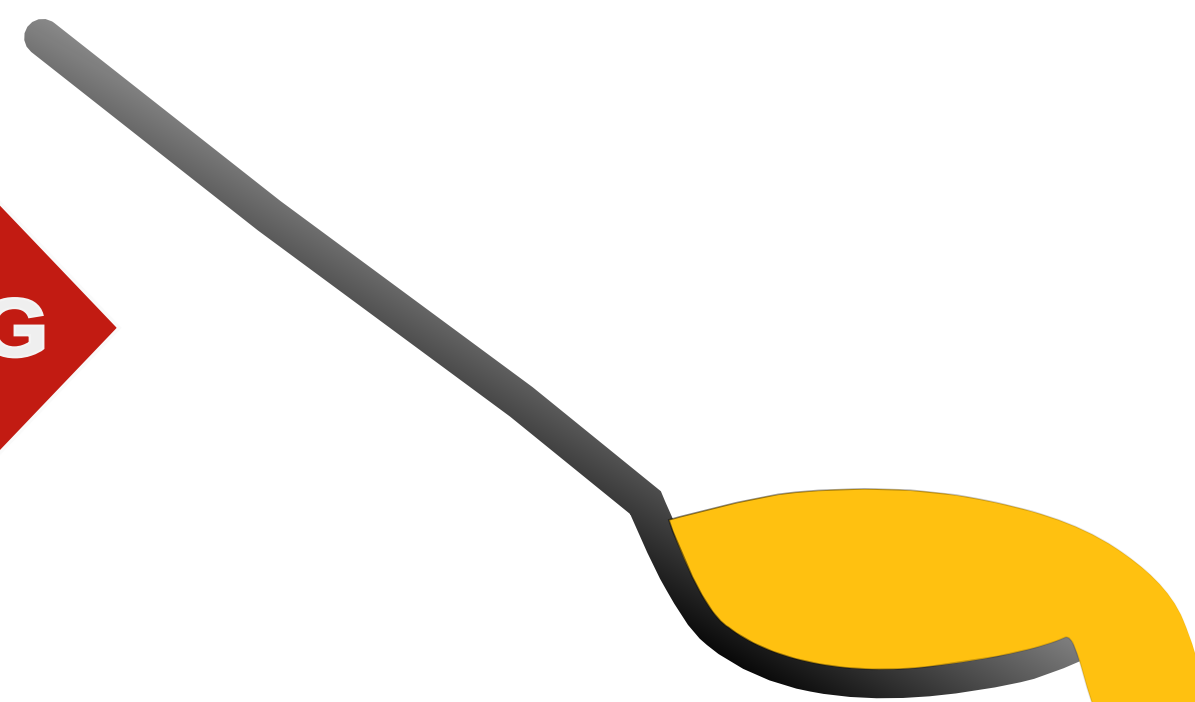


**Highly branched pectins**

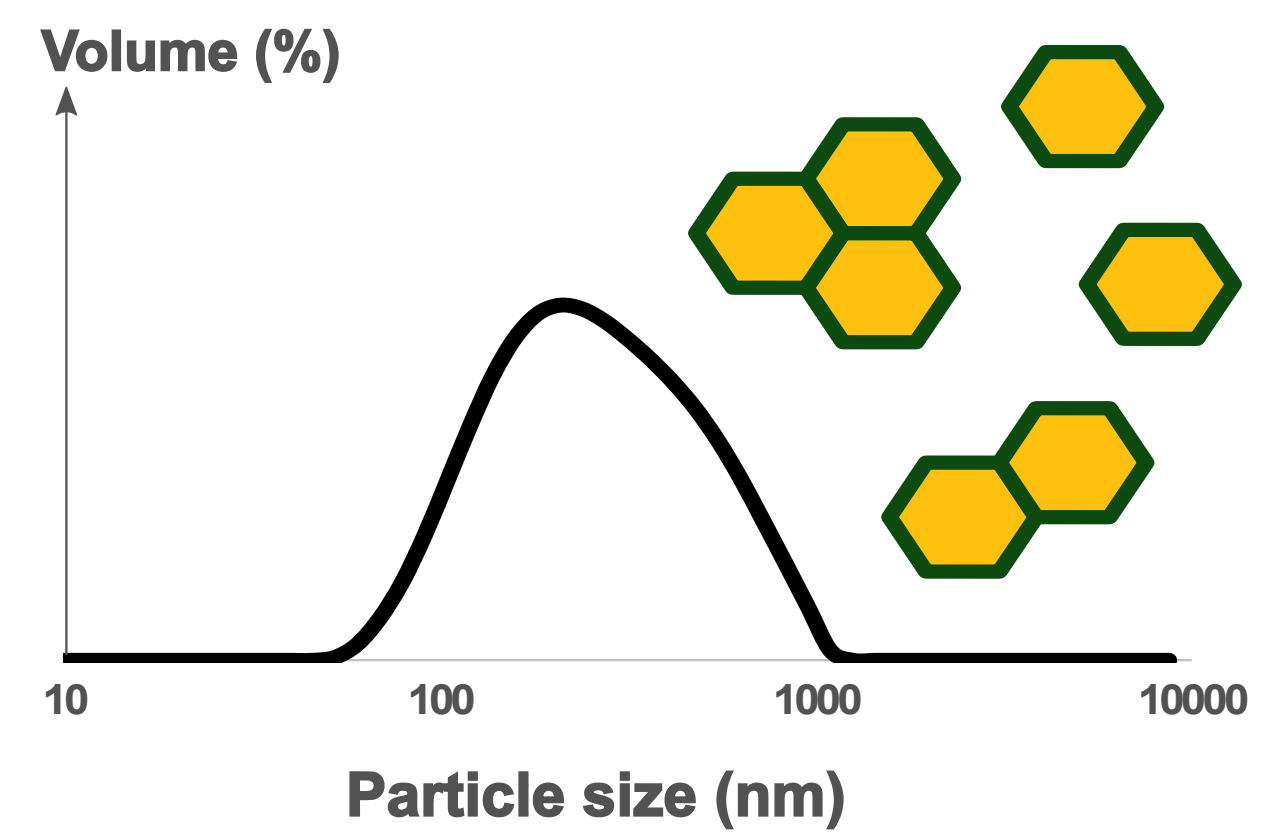


**Prolonged  
storage time**

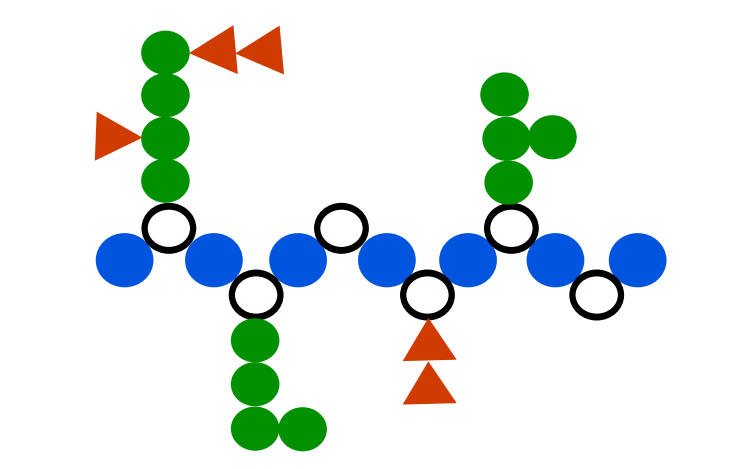
**PROCESSING**



**Low viscosity  
of the apple puree**



**Small cell fragments**



**Less branched pectins**